Enantioselective synthesis of vicinal (R,R)-diols by yeast butanediol dehydrogenase

Eduard Calam, Eva González-Roca, M Rosario Fernández, Sylvie Dequin, Xavier Parés, Albert Virgili, Josep A Biosca

Enantioselective synthesis of vicinal (*R*,*R*)-diols by yeast butanediol dehydrogenase.

Running title: Biotechnological applications of yeast Bdh1p.

Eduard Calam, Eva González-Roca[1], M. Rosario Fernández, Sylvie Dequin[2], Xavier Parés, Albert Virgili[3] and Josep A. Biosca*

Department of Biochemistry and Molecular Biology, Universitat Autònoma de Barcelona, E-08193 Bellaterra (Barcelona). 1 Present address Autoinflammatory Disease Unit Immunology Service (CDB-IDIBAPS) Hospital Clinic (Barcelona) 2 Laboratoire de Microbiologie et Technologie des Fermentations, INRA-IPV, F-34600 Montpellier, France and 3 Department of Chemistry, Universitat Autònoma de Barcelona, E-08193 Bellaterra (Barcelona).

*Correspondence to: Josep A. Biosca, Dept. of Biochemistry and Molecular Biology, Faculty of Biosciences, Universitat Autònoma de Barcelona, E-08193 Bellaterra (Barcelona) Spain

Telefax: 34-93-581 1264

Telephone: 34-93-581 3070

E-mail: josep.biosca@uab.es

Abstract.

Butanediol dehydrogenase (Bdh1p) from *Saccharomyces cerevisiae* belongs to the superfamily of the medium chain dehydrogenases/reductases and converts reversibly *R*-acetoin and *S*-acetoin to (2*R*,3*R*)-2,3-butanediol and *meso*-2,3-butanediol, respectively. It is specific for NAD(H) as a coenzyme and it is the main enzyme involved in the last metabolic step leading to (2*R*,3*R*)-2,3-butanediol in yeast. In this study, we have used the activity of Bdh1p, in different forms: purified enzyme, yeast extracts, permeabilized yeast cells, and as a fusion protein (with yeast formate dehydrogenase, Fdh1p) to transform several vicinal diketones to the corresponding diols. We have also developed a new variant of the "delitto perfetto" methodology to place *BDH1* under the control of the *GAL1* promoter, resulting in a yeast strain that overexpresses butanediol dehydrogenase and formate dehydrogenase activities in the presence of galactose and regenerates NADH in the presence of formate. While the use of purified Bdh1p allows the synthesis of enantiopure (2*R*,3*R*)-2,3-butanediol, (2*R*,3*R*)-2,3-pentanediol, (2*R*,3*R*)-2,3-hexanediol and (3*R*,4*R*)-3,4-hexanediol, the use of the engineered strain (as an extract or as permeabilized cells), yields mixtures of the diols. The production of pure diol stereoisomers has also been achieved by means of a chimeric fusion protein combining Fdh1p and Bdh1p. Finally, we have determined the selectivity of Bdh1p towards the oxidation/reduction of the hydroxyl/ketone groups from (2*R*,3*R*)-2,3-pentanediol/2,3-pentanedione and (2*R*,3*R*)-2,3-hexanediol/ 2,3-hexanedione. In conclusion, Bdh1p is an enzyme with biotechnological interest that can be used to synthesize chiral building blocks. A scheme of the favored pathway with the corresponding intermediates is proposed for the Bdh1p reaction.

Introduction

Biocatalytic transformations using pure enzymes or whole-cell microorganisms offer mild and environmentally benign reaction conditions as opposed to the chemical processes that use harsh conditions and produce residual metals. Several diols, as 1,3-propanediol, 1,2-propanediol, 2,3-butanediol and 1,4-butanediol, are considered platform chemicals because of their many applications in the industry, including the synthesis of special chemicals and their use as precursors of polymers (1). Thus, 2,3-butanediol (2,3-BD) has been used as an antifreeze agent (the stereoisomeric form (2*R*,3*R*)-2,3-BD has a freezing point of -60 °C) and as a precursor of several compounds, through reactions of dehydration (obtaining methyl ethyl ketone, that can be used as a fuel additive), dehydrogenation (giving flavoring compounds as acetoin and diacetyl), ketalization (yielding a potential gasoline blending agent) and esterification (giving precursors of drugs and plasticizers) (2-3, for recent reviews). Several microbial systems have been optimized (by genetic engineering and by optimization of the fermentation conditions) for the production of 2,3-BD, such as *Klebsiella pneumoniae* (4) *Klebsiella oxytoca or Paenibacillus polymyxa* (2) and *E.coli* (5). The manipulation of the carbon flux and cofactor regeneration in *Bacillus amyloliquefaciens*, has resulted in a high-titer of 2,3-butanediol from biodiesel-derived glycerol (6). Recent work has also established the potential of some acetogenic bacteria to produce 2,3-butanediol using CO and/or CO_2 plus H_2 (7). *Saccharomyces cerevisiae* has also been used recently as a producer of 2,3-BD through genetic engineering (8-9). Thus, a pyruvate decarboxylase yeast mutant was used as a starting strain, that was

evolved for rapid glucose consumption, such that the resulting strain achieved 96.2 g/L of 2,3-butanediol production in the fermentation medium (8).

The pure stereoisomers of 2,3-butanediol, (2*S*,3*S*)-, (2*R*,3*R*)- and *meso*- are useful as auxiliaries and can serve as building blocks in the asymmetric synthesis of chiral compounds with two stereogenic centers (10). The three stereoisomeric forms can be produced by microbial fermentation. Thus, (2*R*,3*R*)-2,3-BD can be obtained in high purity from sucrose fermentations by *Paenibacillus polymyxa* (11) and by metabolic engineering of *E. coli* and *S. cerevisae*, through the introduction of biosynthetic pathways composed of endogenous and foreign genes (12-13). (2*S*,3*S*)-2,3-BD has been obtained recently by fed-batch bioconversion from diacetyl using an *E. coli* strain expressing 2,3-BD dehydrogenase and glucose or formate dehydrogenases as cofactor-regenerating systems (14). *meso*-2,3-BD has been produced from a metabolically engineered *E.coli* from glucose fermentation under low oxygen (15). Several classes of oxidoreductases, belonging to the superfamilies of medium chain dehydrogenases/reductases (MDR), aldoketo reductases and short-chain dehydrogenases/reductases have been used in those organisms to convert diacetyl and/or acetoin to 2,3-BD (16-17). A recent biotechnological use for Bdh1p from *Bacillus subtilis* was the production of (3*R*)-acetoin and (3*S*)-acetoin with high enantiomeric excess, from (2*R*,3R)-2,3-butanediol and *meso*-2,3-butanediol respectively (18). They used Bdh1p together with an NAD^+-regenerating system, formed by NADH oxidase from *Lactobacillus brevis* to regenerate NAD^+ from NADH by reducing O_2 to H_2O.

We have previously characterized Bdh1p as an MDR that can reversibly convert *R*-acetoin and *S*-acetoin to (2*R*,3*R*)-2,3-butanediol and *meso*-2,3-

butanediol, respectively using NAD(H) as a coenzyme (19). We have also shown that Bdh1p is the main enzyme involved in the last metabolic step leading to (2*R*,3*R*)-2,3-butanediol in yeast (20). In the present work we have used the activity of Bdh1p in different conditions: (I) purified enzyme, (II) yeast extracts, (III) permeabilized yeast cells and, (IV) as a fusion protein with yeast formate dehydrogenase (Fdh1p), to transform diacetyl, 2,3-pentanedione, 2,3-hexanedione and 3,4-hexanedione to the corresponding diols. By using purified Bdh1p (together with exogenous Fdh to regenerate NADH) we have obtained enantiopure (2*R*,3*R*)-2,3-butanediol, (2*R*,3*R*)-2,3-pentanediol, (2*R*,3*R*)-2,3-hexanediol and (3*R*,4*R*)-3,4-hexanediol. We have also engineered a yeast strain (by developing a new variant of the "delitto perfetto" methodology (21) that overexpresses Bdh and Fdh activities in the presence of galactose. The use of this engineered strain allowed obtaining several diols from the corresponding diketones in the presence of formate, without the need of a coenzyme-regenerating system. Although the use of yeast extracts or permeabilized cells from this strain did not allow the production of pure stereoisomers, we could separate and identify the hydroxyketones and diols arising from the reduction of the diketones. To allow the production of pure diol stereoisomers and to avoid the need of a coenzyme regenerating system, we have constructed a chimeric fusion protein combining Fdh1p and Bdh1p. Finally, we propose a mechanism to explain the selectivity shown by Bdh1p towards the oxidation/reduction of the hydroxyl/ketone groups from (2*R*,3*R*)-2,3-pentanediol/2,3-pentanedione and (2*R*,3*R*)-2,3-hexanediol/ 2,3-hexanedione.

Materials and Methods

Materials.

Restriction enzymes and T4 DNA ligase were from Roche (Basel, Switzerland). Vent and KOD polymerases were from New England Biolabs, Inc. (Beverly, USA) and Merck (Nottingham, United Kingdom) respectively. DNA oligomers were synthesized and purified by Sigma-Genosys (Haverhill, United Kingdom). Chemicals were purchased from Fluka or, Sigma-Aldrich (Saint Louis, USA). *S.cerevisiae* alcohol dehydrogenase and *Candida boidinii* formate dehydrogenase were from Sigma-Aldrich.

Synthesis and NMR analysis of 2,3-pentanediol stereoisomers.

To a stirred solution of 2,3-pentanedione (0.50g, 5 mmols) in methanol (40 ml) a suspension of sodium borohydride (0.180 g, 4.8 mmols) in methanol (20 ml) was added during 60 min. After stirring for 3 hours, the solvent was gently evaporated and the residue was treated with water (50 ml), neutralized and extracted with chloroform (3x30 ml). The solvent was removed obtaining 0.47g (4.5 mmols, 90% yield) of 2,3-pentanediol. The residue was analyzed by ^{1}H- and ^{13}C-NMR. To prepare (2*R*,3*R*)-2,3-pentanediol, we prepared a reaction mixture containing 48 mM 2,3-pentanedione, 1 mM NADH, 100 mM sodium formate, 25 U of Fdh and 10 U of Bdh1p. The mixture was allowed to react for 23 hours and then was extracted with chloroform. The chloroform was evaporated with a rotavapor and the oily extract was dissolved in deuterated chloroform before being analyzed by ^{1}H-NMR.

Yeast and bacterial strains.

Escherichia coli XL-1 blue (Stratagene, La Jolla, USA) or DH5α was used for cloning experiments. The *S. cerevisiae* strains used in this study were derived from the wild type FY834α (*MATα*, *his3Δ200*, *ura3-52*, *leu2Δ1*, *lys2Δ202*, *trp1Δ63*) (22) and from the Adh$^-$ strain WV36-405 (*MAT***a,** *ura3-52, trp1, Δadh1, Δadh2, Δadh3, adh4::TRP1*) constructed by Dr. Wolfgang Vogel (Neuherberg, Germany). Mutant strain EG2 (FY834α *MATα his3Δ200 ura3-52 leu2Δ1 lys2Δ202 trp1Δ63 TRP1::bdh1*) (19) was used to characterize additional NADH dependent diacetyl reductases. Yeast strains deleted for *bdh1* (*Δbdh1*) and/or *ara1* (*Δara1*) were constructed by the one-step gene replacement method (23) with a fragment containing the *kanMX4* and/or *natMX4* (24-25) genes flanked by sequences identical to *BDH1* and/or *ARA1* (20).

Plasmids, DNA manipulations, cloning techniques and transformation methods.

All DNA manipulations were performed under standard conditions as described (26). *E. coli* plasmid DNA was obtained by using a commercial kit provided by Sigma. The plasmids used to overexpress Bdh1p (pYES2-*BDH1*) and Bdh1p-$(His)_6$ (pYES2-*BDH1*-6His) have already been described (19-20). The formate dehydrogenase gene (*FDH1*) from *S. cerevisiae* was amplified from yeast genomic DNA in a PCR with the oligos o-FDH-fw and o-FDH-rv (Table 1). The band containing *FDH1* was excised from an agarose gel, digested with *Bam*HI and *Eco*RI and cloned in the pYES2 vector digested with the same enzymes. The construct pYES2-*FDH1* was sequenced to verify that no mutations had been introduced during the PCR. Plasmids pYES2-*BDH1*-6His and pYES2-*FDH1* (see above) were used as starting points to construct

the plasmid pYES2-*FDH1-BDH1*-6His, expressing the fusion protein containing Fdh1p in its N-terminus and Bdh1-$(His)_6$p in its C-terminus linked by the heptapeptide (ENLYFQG). The gene coding for the fusion protein was constructed in two steps: firstly, we used the oligonucleotides o-FDH-fw and FPint-Rv (Table 1) together with the plasmid pYES2-*FDH1* as a template, which in a PCR resulted in a fragment containing *FDH1* fused to the sequence coding for the peptide linker (see above). Secondly, the oligos FPint-Fw and bdh1-his together with the plasmid pYES2-*BDH1*-6His as a template, were used to construct by PCR a fragment that contained the sequence coding for Bdh1p-$(His)_6$ fused to the aforementioned peptide linker. A mixture of these two fragments, containing a complementary region (underlined in the oligos, see Table 1), was used as template in a PCR with the external oligos o-FDH-fw and bdh1-his to obtain the complete gene coding for the fusion protein Fdh1p-Bdh1p$(His)_6$. The amplified fragment was excised from an agarose gel and cloned in pYES2 digested with *Bam*HI and *EcoR*I. The correctness of the construct was verified by sequencing.

The plasmids were introduced into the yeast strains by the lithium acetate method (23), and the transformants were selected on SC-Ura medium supplemented with 2% glucose or galactose (in the case of the Adh^- strains).

Construction of a yeast strain overexpressing Bdh1p and Fdh1p by self-cloning.

A slight modification of the *delitto perfetto* technique (21) was performed to place *BDH1* under the control of the *GAL1* promoter in its chromosomal *locus*. The promoter and part of the *BDH1* coding region from the

yeast strain WV36-405 were deleted with a double marker (consisting of *URA3* from *Kluyveromices lactis* fused to *natMX4* from *Streptomyces noursei*) obtained by PCR using the plasmids pUG72 and pAG25 (obtained from Euroscarf) as templates. The oligonucleotides used to amplify the double marker by PCR were Pbdh-ura-fw and Bdh-nat1-rv (Table 1). The linear fragment obtained upon PCR (containing two flanking regions identical to the −520→ −473 and +1→ +48 sequences from *BDH1* and its promoter) was used to transform the yeast strain WV36-405 by the lithium acetate method, and the transformants were selected on YPD agar medium (1% Bacto yeast extract, 2% Bacto peptone, 2% glucose-containing 2% agar) supplemented with 100 µg/ml clonNAT (Hans-Knöll Institute für NaturstonForschung, Jena, Germany). Several transformants that grew on clonNAT medium were checked by PCR to verify that the double marker was in the proper place, thus a yeast strain WV36-405 *URA3-NAT1::*P_{bdh1}*-bdh1* was constructed. One of the transformants was grown in SC-Ura medium and transformed with a recombinogenic linear fragment containing the *GAL1* promoter flanked by the −520→ −473 sequence of the *BDH1* promoter and by the +1→+48 sequence from *BDH1*. This fragment had been obtained in a PCR with the oligos: Pbdh-gal-Fw and Bdh-gal-bis-rv (Table 1) by using pYES2-*BDH1* as a template. Upon transformation by the lithium acetate method, the mixture was plated on a YPD plate overnight. The plate was replica plated on a SC plate containing 100 µg/ml uracil and supplemented with 1 mg/ml 5-FOA (27), the following day to allow for counter-selection. The colonies that grew in this plate were replica-plated on a YPD plate containing clonNAT, to discard spontaneous mutations of *URA3* that allowed cells to grow on the 5-FOA plate. Several transformants growing on

Applied and Environmental Microbiology

FOA, but not on clonNAT plates, were checked by PCR with oligos o-gal1-fw and o-bdh1-rv (Table 1) and one of the transformants was verified by sequencing. The new strain (WV36-405 P_{bdh1}::P_{GAL1}-*BDH1*) was transformed with plasmid pYES2-*FDH1* and selected on SC-Ura plates, obtaining a yeast strain named DP-BDH1 overexpressing Bdh1p (because of the presence of its engineered chromosomal *GAL1* promoter controlling *BDH1*) and Fdh1p (under the control of the *GAL1* promoter contained in the pYES2 plasmid) on galactose. Crude extracts were prepared from this strain grown in SC-Ura medium plus 2% galactose until the beginning of the stationary phase. Permeabilized yeast DP-BDH1 cells were prepared by adding 0.1% (w/v) digitonin to the cell suspension, essentially as described (28).

Media and growth conditions.

E.coli was grown at 37°C in Luria-Bertani medium supplemented with 50 µg/ml of ampicillin to select for the desired plasmid constructs. The yeast strains derived from WV36-405 containing pYES2 derived plasmids were grown at 28 °C on a rotatory shaker (250 rpm) in SC-Ura supplemented with 2% galactose.

Bdh1p, Bdh1p(His)$_6$ and Fdh1p-Bdh1(His)$_6$ purification. Molecular mass determination.

Bdh1p, Bdh1p(His)$_6$ and Fdh1p-Bdh1(His)$_6$ were purified from the yeast strains WV36-405 *Δara1* [pYES2-*BDH1*], WV36-405*Δara1 Δbdh1* [pYES2-*BDH1(His)6*] and WV36-405*Δara1 Δbdh1* [pYES2-*FDH1-BDH1*-6His] respectively, as described (19-20). The last step of the purification protocol served to determine the Mr of the fusion protein, Fdh1p-Bdh1p(His)$_6$ by gel-

filtration chromatography. A Hi-Load (26/60) SuperDex 200 prep grade column from GE Healthcare equilibrated with 50 mM Hepes, pH 7 and 150 mM NaCl was used. The column was eluted at a flow rate of 1.75 mL/min with the equilibration buffer.

Enzyme activities, chemical transformations, and coenzyme regenerating systems.

Enzyme activities were determined spectrophotometrically by measuring the change of absorbance at 340 nm and 25°C, corresponding to the oxidation of NADH (ε340 = 6220 M−1· cm−1). One unit (U) of activity corresponds to 1 μmol of NAD+ formed per minute. To determine the steady-state parameters, the initial velocities were measured in duplicate at eight different substrate concentrations and the k_{cat} and K_M for the different substrates (Table 2) were determined by using the nonlinear regression program Grafit 5.0 (Erithacus Software Ltd., Horley, U.K.). All reported values are expressed as the mean ± S.E. of at least three separate experiments. The specific activity of Bdh1p was measured in 33 mM sodium phosphate buffer at pH 7, in the presence of 50 mM (*R*/*S*)-acetoin and 0.2 mM NADH. To ascertain the stereoselectivities of the enzymes, reaction mixtures were prepared in 5 mL tubes with O-ring from Nirco (Barberà del Vallés, Spain) with continuous agitation at room temperature. The initial composition of the mixtures when using pure Bdh1p were 50 mM diketone, 200 U of Bdh1p, 1 mM NADH in 33 mM sodium phosphate, pH 7 buffer and an NADH-regenerating system containing 100 mM sodium formate and 4 U of formate dehydrogenase from *Candida boidinii* (29). When using crude extracts, yeast strain DP-BDH1 (WV36-405 P_{GAL1}-*BDH1* [pYES2-*FDH1*])

was grown in SC-Ura plus galactose until the beginning of the stationary phase and the pelleted cells were disrupted with glass beads. The extracts, containing 150 U of Bdh1 and 3 U of Fdh activities, were incubated with 50 mM diketone together with 1 mM NADH and 100 mM formate. Yeast cells, permeabilized with 0.1 % digitonin (28), were used to drive the reduction of 50 mM diketone, in the presence of 2% galactose, 1 mM NADH, 100 mM formate and 33 mM sodium phosphate pH 7. When using the fusion protein Fdh1p-Bdh1p(His)$_6$, the reaction solution contained 39 U of Bdh and 0.3 U of Fdh, which were incubated with 50 mM diketone together with 5 mM NAD^+ and 100 mM formate as an NADH-regenerating system. For the oxidation of the diols with pure Bdh1p, we used an NAD^+ regenerating system containing α-ketoglutarate, ammonium chloride and glutamate dehydrogenase in 33 mM sodium phosphate buffer at pH 7 (29).

Western blots and in-gel assays of Bdh activity of yeast extracts.

Bdh1p(His)$_6$ and Fdh1p-Bdh1(His)$_6$ expressed from WV36-405*Δara1 Δbdh1* [pYES2-*BDH1*-6His] and WV36-405*Δara1BDH1*[pYES2-*FDH1-BDH1*-6His] yeast strains were detected by Western blotting using a mouse monoclonal anti-His$_6$ antibody following a previously described method (20).

Yeast protein extracts from strains expressing Bdh1p(His)$_6$ and Fdh1p-Bdh1(His)$_6$ in different genetic backgrounds were loaded on precast (pH 3 to 9) IEF gels from Bio-Rad (Criterion). Their Bdh activities were visualized on the gels by incubating them with 100 mM (2R,3R)-2,3-butanediol, 2 mM NAD^+, together with 0.08 mg/ml of phenazine methosulfate, and 0.8 mg/ml of nitroblue tetrazolium, essentially as described (20).

Analytical methods.

The reaction mixtures were extracted with chloroform, to recover the hydroxyketones and diols, together with 1-hexanol, as an internal standard, essentially as described (30). A slight modification was introduced to quantify *R*- and *S*-acetoin and the different 2,3-butanediol stereoisomers obtained from the overnight reaction mixtures. To 1-mL reaction mixture, 1-hexanol was added up to 8 mM, together with 2.5 g of K_2CO_3, followed by two successive extractions with 2 and 4 mL chloroform. Both extractions were necessary to attain linearity in the recovered acetoins and 2,3-butanediols from standard additions to the reaction mixtures. Alternatively, the analytes were extracted from the reaction mixtures with two successive ethyl acetate extractions (19). The different stereoisomers of the hydroxyketones and diols were resolved on a chiral column (Supelco β-DEX ™ 120, 30 m length, 0.25 mm inner diameter), coupled to a Hewlett-Packard gas chromatograph equipped with a mass spectrophotometer as a detector, under conditions previously described (19). The identity of the products was verified by known standards (when available) and by mass spectrometry. To confirm the resolution between (3*R*)-hydroxy-2-pentanone and (2*R*)-hydroxy-3-pentanone, we also used an HP-5MS Agilent column, 30 m length, 0.25 mm inner diameter, coupled to a Hewlett-Packard gas chromatograph equipped with a mass spectrophotometer as a detector. The following temperature program was used: isotherm at 45°C for 2 min and three ramps 5°C/min up to 100°C, 15°C/min up to 150°C and 30 °C/min up to 275°C. The identity of the products was verified by mass spectrometry.

Results

Kinetic parameters and stereoselectivity of Bdh1p.

Table 2 gives the kinetic parameters determined for Bdh1p towards acetoin, diacetyl, 2,3-pentanedione, 2,3-hexanedione and 3,4-hexanedione. The specificity constant k_{cat}/K_M decreased from acetoin to 2,3-hexanedione and then increased for 3,4-hexanedione. The reaction of purified Bdh1p with diacetyl specifically produced (2*R*,3*R*)-2,3-butanediol, with a 95% yield, and a minor amount of *R*-acetoin (Fig 1A). To determine the stereoisomeric purity of the (2*R*,3*R*)-2,3-butanediol obtained, we added a known concentration of *meso*-2,3-butanediol and (2*S*,3*S*)-2,3-butanediol to half of the reaction mixture obtained upon the reaction of Bdh1p with diacetyl (and the NADH-regenerating system). An equal volume of buffer was added to the other half of the reaction. By comparing the areas of the known added concentrations of *meso*-2,3-butanediol and (2*S*,3*S*)-2,3-butanediol (panel B in Figure 2) and the corresponding ones in panel A, we estimated a stereoisomeric purity of (2*R*,3*R*)-2,3-butanediol greater than 99.6% (Fig 2).

When using Bdh1p with 2,3-pentanedione, 2,3-hexanedione and 3,4-hexanedione only one diol was obtained (Fig 1B, C, D), identified as 2,3-pentanediol, 2,3-hexanediol and 3,4-hexanediol, respectively, by their mass spectra. Since there are not commercial sources of pure stereoisomers of these compounds that could be used as standards, we assigned the configuration of the stereoisomer of 2,3-pentanediol produced by Bdh1p, by comparing the ^{1}H-NMR spectrum obtained from 2,3-pentanediol obtained chemically with the one from the diol obtained with pure Bdh1p (Supplemental Fig S1).

The ^{1}H and ^{13}C-NMR spectra of chemically prepared 2,3-pentanediol showed the presence of two diastereoisomers, (2*RS*,3*RS*) and (2*RS*,3*SR*) in their racemic form, showing a good agreement with NMR data described before (31). Thus, the pair (2*R*,3*S*) plus (2*S*,3*R*) [abbreviated (2*RS*,3*SR*)] showed the chemical shifts at δ=3.81ppm (for the H-2), δ=3.55 (for the H-3), δ=1.15 (for the H-1) and δ=1.00 (for the H-5) (supplemental Fig 1, panel B). In its turn, the pair (2*R*,3*R*) plus (2*S*,3*S*) [abbreviated (2*RS*,3*RS*)] showed the chemical shifts at δ=3.61ppm (for the H-2), δ=3.27 (for the H-3), δ=1.20 (for the H-1) and δ=1.00 (for the H-5) (supplemental Fig S1, panelB). From the areas of the corresponding signals, the two isomers were obtained in a ratio of 2.14 being the isomers (2*RS*, 3*SR*) the major compounds (Supplemental Fig S1, panel B). When the same mixture of 2,3-pentanediols was loaded in a GC equipped with a chiral column, the four stereoisomers were resolved, being those eluting at t_R=14.86 and 15.51 minutes less abundant than the other two (supplemental Figure S2). In consequence, these minority stereoisomers should correspond to the pair (2*RS*, 3*RS*).

Moreover, when we prepared 2,3-pentanediol by the action of Bdh1p and the NADH-regenerating system, only one 2,3-pentanediol stereoisomer was obtained, eluting at 15.56 minutes (supplemental Figure S3) and with a NMR spectrum coincident with the one from the pair (2*RS*, 3*RS*). The chemical shifts for this compound were at δ=3.58 ppm (for the H-2), δ=3.24 (for the H-3), δ=1.17 (for the H-1) and δ=0.98 (for the H-5) (supplemental Fig S1, panel A). Since the NMR signals obtained for this compound are coincident with the ones from the pair (2*RS*, 3*RS*), this stereoisomer should be (2*R*,3*R*)-2,3-pentanediol or (2*S*,3*S*)-2,3-pentanediol. Given the stereoselectivity displayed by Bdh1p

375 towards diacetyl, we assign the peak eluting at 15.51 minutes to (2*R*,3*R*)-2,3-
376 pentanediol (also see Discussion) and automatically the stereoisomer eluting at
377 t_R=14.86 to (2*S*,3*S*)-2,3-pentanediol (supplemental Figure S2).
378
379 **Search for other yeast NADH-dependent diacetyl reductases.**
380 A protein extract of a yeast strain deleted for *bdh1*, namely EG2
381 (FY834α *TRP1::bdh1*) (19) grown in YPglucose displayed a diacetyl reductase
382 activity of 0.73 U/mg (measured in 50 mM diacetyl and 0.2 mM NADH). The
383 extract was loaded in an IEF gel and the diacetyl reductase activities were
384 visualized by activity staining with diacetyl and NADH (results not shown). A
385 clear band with a pI lower than the pI of Bdh1p (Bdh1p was not visible in this gel
386 since *BDH1* was disrupted in the strain EG2) indicated that another enzyme (or
387 enzymes) was able to reduce diacetyl in an NADH- dependent reaction.
388 Therefore, we developed a protocol to purify this diacetyl reductase activity from
389 the yeast strain EG2. The protocol consisted of a DEAE-Sepharose, followed by
390 a hydroxyapatite column and by a Cibachron Blue 3GA chromatography. We
391 obtained a homogeneous protein with an estimated Mr of approximately 42,000
392 (by SDS-PAGE), which upon digestion with trypsin was analyzed by MALDI-
393 TOF MS (conditions described in González et al., 2010). The protein was
394 identified as Adh2p, and thus we analyzed by GC-MS the products obtained in
395 the reduction of diacetyl in the presence of Adh2p, which resulted in *S*-acetoin.
396 Given the similarity between Adh2p, Adh1p and Adh3p, we cloned and over-
397 expressed Adh1p and Adh3p (by means of the galactose inducible pYES2
398 vector) in the WV36-405 strain, finding that both displayed diacetyl reductase
399 activity, also yielding *S*-acetoin. The supplemental Figure S4 shows that

diacetyl treated with yeast Adh yielded S-acetoin. When the filtrate obtained upon this reduction, was treated with Bdh1p, meso-2,3-butanediol was obtained (supplemental Figure S5). Moreover, when 2,3-pentanedione was treated with yeast Adh yielded (2*S*)-hydroxy-3-pentanone (supplemental Figure S6). When the filtrate obtained upon this reduction, was treated with Bdh1p, (2*S*,3*R*)-2,3-pentanediol was obtained (supplemental Figure S7). The residual amount of 2,3-pentanedione from the filtrate yielded (3*R*)-hydroxy-2-pentanone and (2*R*,3*R*)-2,3-pentanediol (supplemental Figure S7). Thus, since Bdh1p is enantioselective yielding (*R)*-acetoin from diacetyl and, (2*R*,3*R*)-2,3-butanediol from (*R*)-acetoin, we decided to use the Adh-deficient strain WV36-405 when working with extracts and permeabilized cells to minimize the production of *S*-acetoin, that would yield *meso*-2,3-butanediol upon the action of Bdh1p.

Diols and hydroxyketones obtained from vicinal diketones by yeast extracts and permeabilized cells.

Although purified Bdh1p yields enantiopure vicinal diols upon the reduction of the corresponding diketones, an NADH-regenerating system was necessary to displace the reaction towards the diols. To avoid the need of an external source of FDH activity to regenerate NADH, we constructed a yeast strain that overexpressed Bdh1p and yeast formate dehydrogenase (Fdh1p), such that it would not be necessary to purify Bdh1p, nor the addition of exogenous FDH. As a first step to construct such a strain, we used a modification of the *"delito perfetto"* technique (21) developed in our laboratory to change the chromosomal promoter of *BDH1* by the *GAL1-10* promoter. Then, a multicopy inducible plasmid with cloned *FDH1* under the control of the *GAL1*

promoter was used to transform the previous yeast strain, such that the presence of galactose in the growth medium induced the Bdh and Fdh activities. The resulting yeast strain was named DP-BDH1 (WV36-405 P_{GAL1}-*BDH1* [pYES2-*FDH1*]). To ascertain the overexpression of Bdh and Fdh activities in the strain DP-BDH1, we grew it and its parental control strain (WV36-405 P_{BDH1}-*BDH1* [pYES2]) in galactose containing medium. At the end of their logarithmic phases, we obtained the yeast extracts by disrupting the cells with glass beads and determined their Bdh and Fdh activities. While the Bdh and Fdh specific activities from the control strain, WV36-405 P_{BDH1}-*BDH1*[pYES2], were 0.26 and less than 0.001 U/mg, respectively (measured at 5 mM NAD^+ and 100 mM (2*R*,3*R*)-butanediol or 100 mM formate), the corresponding ones from the strain DP-BDH1 were 1.22 and 0.13 U/mg, respectively. The yeast strain DP-BDH1 was permeabilized with 0.1% digitonin, following the technique of Cordeiro and Freire (1995) and incubated with the different diketones and galactose containing medium. When using the protein extracts or the digitonin permeabilized yeast cells DP-BDH1, grown in galactose, on the different diketones, the products obtained were a mixture of all possible stereoisomers (Figs. 3 and 4). Thus, (2*R*,3R)-2,3-butanediol, *meso*-2,3-butanediol and traces of (2*S*,3*S*)-2,3-butanediol were the products upon the reduction of diacetyl with permeabilized cells with a yield of 65% (adding the 3 butanediol stereoisomers) (Fig. 4). Furthermore, the additional enzymatic activities present in the yeast extracts and permeabilized cells yielded several diol stereoisomers from 2,3-pentanedione, 2,3-hexanedione and 3,4-hexanedione (Figs. 3 and 4). For instance, the four stereoisomers of 2,3-

hexanediol could be detected from their mass spectra, upon the reaction of 2,3-hexanedione with DP-BDH1 extracts or permeabilized cells (Figs. 3C and 4C).

Identification of the stereoisomeric forms of the hydroxyketones and vicinal diols.

In the case of the acetoin and 2,3-butanediol stereoisomers obtained upon reduction of diacetyl (Figs. 3A and 4A), the assignation of the stereoisomeric forms was made by comparison with the retention times of the pure (2*R*,3*R*)-2,3-butanediol, *meso*-2,3-butanediol and (2*S*,3*S*)-2,3-butanediol and also after the oxidation of pure (2*R*,3*R*)-2,3-butanediol to *R*-acetoin (19) and of *meso*-2,3-butanediol to *S*-acetoin. In the case of 2,3-pentanedione (Figure 4B), the MS of the peaks that eluted at 7.06 and 7.77 min (*m/z* of 59, 43 and 31, in decreasing % abundance) identified them as 3-hydroxy-2-pentanones (32), while the peak eluting at 7.64 min (*m/z* of 45, 57 and 43, in decreasing % abundance) was identified as 2-hydroxy-3-pentanone (32). The stereoisomeric form eluting at t_R=7.06 min was assigned to (3*R*)-hydroxy-2-pentanone since its retention time was the same as the product obtained with pure Bdh1p and 2,3-pentanedione (after one hour of reaction only). Thus, the 3-hydroxy-2-pentanone eluting at 7.77 min must be (3*S*)-hydroxy-2-pentanone. The 2-hydroxy-3-pentanone eluting at 7.64 min was assigned to (2*S*)-hydroxy-3-pentanone, since this retention time was the same as the product obtained upon reduction of 2,3-pentanedione with pure Ara1p (33). Further evidences for the assignments of the hydroxyketones were obtained from the oxidations of (2*R*,3*R*)-2,3-pentanediol and (2*R*,3*R*)-2,3-hexanediol with pure Bdh1p (see below).

The 2,3-pentanediol peaks observed upon reduction of 2,3-pentanedione with yeast extracts or permeabilized cells overexpressing Bdh1p and Fdh1p (Figures 3B and 4B) were assigned according to the signal obtained with pure Bdh1p on 2,3-pentanedione (see above), for (2*R*,3*R*)-2,3-pentanediol (eluting at t_R=16.87 min, Fig 4, panel B). The identities of the stereoisomers (2*R*,3*S*)-2,3-pentanediol and (2*S*,3*R*)-2,3-pentanediol, were established by treating 2,3-pentanedione with Ara1p followed by Bdh1p: by our previous work (33), we knew that (2*S*)-hydroxy-3-pentanone should be obtained from Ara1p and (2*S*,3*R*)-2,3-pentanediol after treating this hydroxyketone with Bdh1p. This compound corresponds to the peak eluting at t_R=18.19 minutes (Fig 4, panel B), so finally the peak eluting at t_R=18.07 minutes should be (2*R*,3*S*)-2,3-pentanediol (Fig 4, panel B). No (2*S*,3*S*)-2,3-pentanediol is observed in these figures.

In regard to the 2,3-pentanediol stereoisomers obtained chemically (supplemental Figure S2), the identities of the different stereoisomers are marked in the figure. The elution times are different from the ones obtained in the reduction of 2,3-pentanedione by yeast extracts (and permeabilized cells) because the reaction mixtures were extracted with ethyl acetate and were run at different days.

The same experimental strategy and reasoning was followed to assign the hydroxyketones and 2,3-hexanediols derived from 2,3-hexanedione (Fig. 4C). First, the four peaks eluting from t_R=20 to 21 min, were assigned to 2,3-hexanediol by their MS (with *m/z* of 55, 73, 45 and 43, in decreasing % abundance), characteristic of 2,3-hexanediols (34). Second, the treatment of 2,3-hexanedione with pure Bdh1p allowed us to assign (2*R*,3*R*)-2,3-hexanediol

to the t_R=20.25 minutes peak, and the treatment of 2,3-hexanedione with Ara1p followed by Bdh1p, allowed to assign (2*S*,3*R*)-2,3-hexanediol to the 20.74 min peak (Fig. 4C). The remaining stereoisomers were assigned as in the case of the reduction of 2,3-pentanedione. In fact, the same order of elution of the 2,3-hexanediols stereoisomers was also obtained by Schröder et al. (1994), working with a β-cyclodextrin chiral column (34).

In the case of the diols produced upon the reduction of 3,4-hexanedione (Fig. 4D), the assignation of the stereoisomeric forms was made as in the case of diacetyl reduction.

Properties of the fusion protein Fdh1p-Bdh1p(His)$_6$.

The fusion protein Fdh1p-Bdh1p(His)$_6$ was purified from the yeast strain WV36-405*Δara1 Δbdh1* [pYES2-*FDH1-BDH1*-6His], by means of a Ni-Sepharose column, followed by gel-filtration on a Hi-Load SuperDex 200 that also served to determine its Mr. The estimated Mr for Fdh1p-Bdh1p(His)$_6$ and Bdh1p(His)$_6$ were 133,000 and 70,500, respectively (Fig. 5C). Given the Mr of Fdh1p (Mr=41,700) and Bdh1p (Mr=41,500) monomers, the active form of the fusion protein is a dimer of two Fdh1-Bdh1(His)$_6$p polypeptides. The fusion protein is rather unstable as it can be deduced from the Western blot analysis (Fig. 5A, lane 2). A main band of an apparent Mr close to 95,000 (consistent with the Mr of a Fdh1p-Bdh1p(His)$_6$ polypeptide) and several bands (presumably degradation products) of lower Mr are visible in the blot. Under these conditions Bdh1p(His)$_6$ is stable as only one band of the correct Mr is visible in the blot (Fig. 5A, lanes 3 and 4). Furthermore, the presence of Fdh1p in the fusion protein decreases the pI of Bdh1p(His)$_6$p (compare lanes 3 and 4 with lane 2 in Fig. 5B). Thus, the activity bands seen in the gel (Fig. 5B, lane 2)

Applied and Environmental Microbiology

confirm that Fdh1p-Bdh1p(His)$_6$ had a lower pI than Bdh1p(His)$_6$ in two genetic backgrounds, with endogenous Bdh1p (Fig 5B, lane 3) and without endogenous Bdh1p (Fig. 5B, lane 4). Moreover, we determined the kinetic constants of Fdh1p-Bdh1p(His)$_6$ towards (*R*/*S*)-acetoin as K_M=2.2 mM (determined at 0.2 mM NADH) and k_{cat}= 31s^{-1}. From the specific activity of Fdh1p-Bdh1p(His)$_6$ towards formate (at 5 mM NAD^+), an apparent k_{cat} of 0.25 s^{-1} was estimated at 25 °C. Thus, the k_{cat} of the fusion protein for acetoin was approximately 50 times lower than the k_{cat} of Bdh1p (Table II), while the K_M values were similar. The k_{cat} for formate was 24 times lower than the published value obtained at 30°C (35).

Hydroxyketones and diols produced by the fusion protein Fdh1p-Bdh1p(His)$_6$.

The purified fusion protein Fdh1p-Bdh1p(His)$_6$ yielded a single form of diol, namely (2*R*,3*R*)-2,3-butanediol, upon diacetyl reduction (Fig. 6A) with a conversion of 31%. Moreover, when starting with either 2,3-pentanedione, 2,3-hexanedione or 3,4-hexanedione a single stereoisomeric form of diol was obtained also (Figs. 6B, C and D). Since these diols have the same retention times than the diols obtained with pure Bdh1p, they have been tentatively assigned as the corresponding (*R*,*R*) stereoisomers. The reduction of the diketones by Fdh1p-Bdh1p(His)$_6$ yielded also hydroxyketones. In the case of diacetyl, the hydroxyketone was identified as *R*-acetoin, while in the case of 2,3-pentanedione and 2,3-hexanedione, they were identified by their mass spectra as 3-hydroxy-2-pentanone and 3-hydroxy-2-hexanone, respectively. We assigned them the *R* configuration (Fig. 6) because we assume that, for these

compounds, the fusion protein displays the same enantioselectivity shown towards diacetyl.

Oxidation of the vicinal diols with Bdh1p.

We first studied the products obtained in the oxidation reaction of (2*R*, 3*R*)-2,3-butanediol by Bdh1p in the presence of NAD^+ and an NAD^+-regenerating system, consisting of α-ketoglutarate, ammonium chloride and glutamate dehydrogenase. We obtained *R*-acetoin as expected from the oxidation of (2*R*,3*R*)-2,3-butanediol (results not shown). Since (2*R*,3*R*)-2,3-pentanediol, (2*R*,3*R*)-2,3-hexanediol and (3*R*,4*R*)-3,4-hexanediol are not commercially available, they were obtained *in situ* from the reaction products upon reduction of 2,3-pentanedione, 2,3-hexanedione and 3,4-hexanedione by Bdh1p (presumably the (*R*,*R*)-stereoisomers, see above). When using (2*R*,3*R*)-2,3-pentanediol and NAD^+ with Bdh1p, together with the NAD^+-regenerating system, one peak was obtained, with a MS pattern compatible with 2-hydroxy-3-pentanone (Fig. 7C). We also analyzed the reaction products obtained upon the reduction of 2,3-pentanedione with Bdh1p (after one-hour reaction) and observed a peak, identified as 3-hydroxy-2-pentanone (Fig. 7A). The insets from Figs. 7A and 7C show only the most abundant and selective ions for (3)-hydroxy-2-pentanone (m/z of 59, black) and (2)-hydroxy-3-pentanone (m/z of 45, red) for clarity. Both compounds should have the *R*-configuration and showed close retention times on the chiral column. We obtained an additional proof of their identities by loading them (as a chloroform extract) on an HP-5MS column, which resolved two peaks corresponding to (3*R*)-hydroxy-2-pentanone and (2*R*)-hydroxy-3-pentanone (results not shown). Furthermore, a mixture of

the four stereoisomeric forms of 2,3-pentanediol was oxidized with Bdh1p and, the most reactive species were (2*R*,3*R*)-2,3-pentanediol, yielding essentially (2*R*)-hydroxy-3-pentanone (t_R= 6.36 min), but also a minor amount of (3*R*)-hydroxy-2-pentanone (t_R= 6.31 min) and, (2*S*,3*R*)-2,3-pentanediol that yielded (2*S*)-hydroxy-3-pentanone (t_R= 6.76 min). A minor amount of (3*S*)-hydroxy-2-pentanone (t_R= 6.91 min) was obtained from the oxidation of (2*R*,3*S*)-2,3-pentanediol by Bdh1p (supplemental Figure S8). We did a parallel study with (2*R*,3*R*)-2,3-hexanediol with similar results. Thus, the reduction of 2,3-hexanedione yielded (3*R*)-hydroxy-2-hexanone (Fig. 8A and C), while the oxidation of (2*R*,3*R*)-2,3-hexanediol yielded (2*R*)-hydroxy-3-hexanone (Fig. 8B and D). Fig 8C and D show only the most abundant and selective ions for 3-hydroxy-2-hexanone (*m/z* of 55, black), and 2-hydroxy-3-hexanone (*m/z* of 45, red). However, since the reduction of 2,3-hexanedione was not complete (Fig 8A), some (3*R*)-hydroxy-2-hexanone was carried over together with (2*R*,3*R*)-2,3-hexanediol, which is visible in the chromatogram (Fig. 8B). With all these data on the oxidation/reduction of vicinal diols/diketones with Bdh1p, we propose as a mechanism that the more reactive carbon upon oxidation (of the diol) and reduction (of the diketone) would be that corresponding to the most internal hydroxyl (or keto) group (Fig. 9). Furthermore, in order to resolve all the stereoisomeric forms of 2-hydroxypentanone and 3-hydroxypentanone (as well as the corresponding hydroxyhexanones), we induced the racemization and isomerization through enolate species of the hydroxyketones by adding NaOH to the products obtained upon oxidation of (2*R*,3*R*)-2,3-pentanediol and (2*R*,3*R*)-2,3-hexanediol (or reduction of the diketones). Figure 10 shows that the chiral column successfully resolved all the hydroxyketone stereoisomers.

Applied and Environmental Microbiology

Discussion

The main aims of the present work were to develop a system able to produce (*R*,*R*) diols from vicinal diketones, to determine the stereoselectivity of Bdh1p towards the reduction of the two carbonyl groups, to determine the kinetic constants of the reactions and to elucidate its preference towards the keto groups of the vicinal diketones. In the first part of the study, we showed that pure Bdh1p reduced both carbonyl groups from diacetyl to stereoisomerically pure (2*R*,3*R*)-2,3-butanediol (Fig. 2A and B). Furthermore, when using 2,3-pentanedione, 2,3-hexanedione and 3,4-hexanedione with pure Bdh1p, only one stereoisomeric form of the corresponding diols was identified in the reaction mixtures. Given the stereoselectivity displayed by Bdh1p towards diacetyl and, since there are not commercial sources of those pure stereoisomers, we tentatively assigned them to the corresponding (*R*, *R*) stereoisomers. We performed, however, NMR and GC experiments to assign the configuration of the 2,3-pentanediol stereoisomer produced by Bdh1p from 2,3-pentanedione. There are several reasons to conclude that the stereoisomer is (2*R*,3*R*)-2,3-pentanediol. Thus, the NMR experiments on the four 2,3-pentanediol stereoisomers obtained chemically show the signals from the pair (2*R*,3*S*) plus (2*S*,3*R*) and the pair (2*R*,3*R*) plus (2*S*,3*S*). The NMR signals show that the pair (2*R*,3*R*) plus (2*S*,3*S*) is in a ratio twice as low as the pair (2*R*,3*S*) plus (2*S*,3*R*). Since the same mixture loaded in a GC show two peaks in a ratio twice as low as the two other peaks, those peaks correspond to the pair (2*R*,3*R*) plus (2*S*,3*S*). Thus, the results from the NMR data alone do not discard a mixture of (2*R*,3*R*)-2,3-pentanediol and its enantiomer (2*S*,3*S*)-2,3-pentanediol, on the reduction of 2,3-pentanedione by Bdh1p (supplemental

Figure S1). However, only one stereoisomer was obtained, when the reaction mixture was loaded in the chiral column (supplemental Figure S2). Consequently, the product can be (2*R*,3*R*)-2,3-pentanediol or (2*S*,3*S*)-2,3-pentanediol. Given the stereospecificity shown by Bdh1p towards the production of (2*R*,3*R*)-2,3-butanediol from diacetyl, the production of pure (2*S*,3*S*)-2,3-pentanediol from 2,3-pentanedione, without any production of the (2*R*,3*S*)-2,3-pentanediol nor (2*S*,3*R*)-2,3-pentanediol seem very unlikely.

The steady-state kinetic studies performed with pure Bdh1p and several vicinal diketones show that the specificity constant k_{cat}/K_M decreased from diacetyl to 2,3-hexanedione and then increased for 3,4-hexanedione (Table 2). Bdh1p displayed the highest specificity constants towards the substrates known to be transformed by Bdh1p in the *Saccharomyces cerevisiae* metabolism: i.e. acetoin, diacetyl and 2,3-pentanedione.

Although the use of pure Bdh1p yielded only one stereoisomeric form of the diols, it was necessary to use formate and exogenous formate dehydrogenase to regenerate NADH. To avoid this drawback, we explored the possibility of using a yeast strain derived from FY834 (22) which could overexpress their endogenous *BDH1* and *FDH1*. To choose a convenient genetic background, we tested first whether there were any diacetyl reductases other than Bdh1p in the yeast extracts derived from the wild type strain FY834. We detected Adh2p with an NADH-dependent reductase activity that yielded *S*-acetoin from diacetyl. Besides, we showed that Adh1p and Adh3p could also reduce diacetyl to *S*-acetoin, in NADH-dependent reactions. Furthermore, with a commercial preparation of yeast Adh, we obtained also *S*-acetoin from diacetyl (supplemental Figure S4). Consequently, we decided to work with a yeast strain

649 with a genetic background *Δadh1, Δadh2, Δadh3* (as WV36-405), to avoid the
650 production of *meso*-2,3-butanediol, that would be obtained from *S*-acetoin by
651 Bdh1p (19) (supplemental Figure S5). We developed a modified *delitto perfetto*
652 technique (21), to overexpress Bdh1p and Fdh1p in the strain WV36-405. The
653 counter-selection marker used, *URA3* from *Kluyveromices lactis*, being different
654 in sequence to *URA3* from *S.cerevisiae,* minimized the homologous
655 recombination events to the endogenous *URA3* locus, while the selection
656 marker *NAT1* yields less spontaneous mutants than the *kanMX4* marker (25).
657 Thus, by placing the *GAL1-10* promoter controlling *BDH1* and transforming the
658 resultant strain with a multicopy galactose-inducible plasmid carrying *FDH1*, we
659 obtained a modified yeast strain (named DP-BDH1) that overexpressed Bdh1p
660 and Fdh1p in the presence of galactose. We measured a 4.5-fold increase in
661 Bdh specific activity towards (2*R*,3*R*)-2,3-BD and more than 100 fold increase in
662 Fdh specific activity towards formate in the corresponding protein extracts, in
663 comparison to the values of the parental strain, transformed with an empty
664 plasmid. We used this engineered strain in the form of protein extracts and
665 permeabilized cells to drive the reductions of diketones without exogenously
666 added Fdh. Although the diketones were reduced, the obtained diols were a
667 mixture of different stereoisomers. Thus, with diacetyl, *meso*-2,3-butanediol and
668 (2*R*,3*R*)-2,3-butanediol were identified as products by using protein extracts or
669 permeabilized cells (Figs. 3 and 4). A mixture of different stereoisomeric forms
670 of 2,3-pentanediol, 2,3-hexanediol and 3,4-hexanediol were obtained in the
671 reductions of 2,3-pentanedione, 2,3-hexanedione and 3,4-hexanedione,
672 respectively (Figs. 3 and 4). Although it was advantageous to use DP-BDH1
673 with no need of coenzyme regenerating processes, the diastereoisomeric

composition of the products precludes its use to obtain pure (*R*,*R*)-diols. Mixtures of stereoisomeric alcohols are formed because of the presence of other enzymes that could convert the same substrates but with different stereoselectivities. Thus, the activities of other diketone reductases (NADH- and also NADPH-dependent in the permeabilized cells) in yeast would be responsible for the production of *S*-hydroxyketones and the different stereoisomeric forms of the diols (20, 32). In fact, the reduction of diacetyl and 2,3-pentanedione for only one hour, allowed the observation of *S*-acetoin, (2*S*)-hydroxy-3-pentanone and (3*S*)-hydroxy-2-pentanone (Fig. 4A and 4B). Then, Bdh1p and/or other reductases would reduce these mixtures of hydroxyketones to the corresponding mixture of diols. A mixture of stereoisomeric alcohols derived from the reduction of α- and β-ketoesters was already observed working with yeast cells (17).

To avoid these interfering activities, and the use of exogenous Fdh, we constructed a bifunctional fusion protein containing Fdh and Bdh activities with a His-tag at its C-terminus Fdh1p-Bdh1p$(His)_6$. By using this protein, pure (2*R*,3*R*)-2,3-butanediol, (2*R*,3*R*)-2,3-pentanediol, (2*R*,3*R*)-2,3-hexanediol and (3*R*,4*R*)-3,4-hexanediol (Fig. 6) were obtained, but with lower yield (31% with (2*R*,3*R*)-2,3-butanediol) than when using pure Bdh1p and exogenous formate dehydrogenase (95% conversion of diacetyl into (2*R*,3*R*)-2,3-butanediol). The fusion Fdh1p-Bdh1p$(His)_6$ behaved as a dimer in a gel-filtration column (Fig. 5C), consistent with the fact that Bdh1p is a dimer (19) and the orthologous formate dehydrogenase from *Candida boidinii* is also a dimer (36). The stability of the fusion protein was checked by Western-blot and zymogram analyses (Fig. 5A and B), showing that the protein suffered proteolysis but maintained

Applied and Environmental Microbiology

699 Bdh activity on the zymogram. The use of this fusion protein allowed the
700 production of pure (*R*,*R*)-diols from vicinal diketones, without the need of adding
701 an external cofactor-regenerating system, but with a low yield. In fact the k_{cat}
702 values of the Bdh and Fdh activities were 50 and 24 times lower, respectively,
703 for the fusion protein than for the individual enzymes. However, this strategy
704 allowed the rapid purification of the fusion protein and the production of
705 enantiopure (*R*,*R*)-diols. However, further work needs to be done, to increase
706 the stability of the fusion protein and the expression level and/or the turnover
707 rate of Fdh1p. A similar approach for cofactor regeneration was used recently
708 by Hölsch and Weuster-Botz (2010) to convert a prochiral ketone to (*S*)-1-
709 (pentafluorophenyl)-ethanol. They used a bifunctional protein composed of an
710 $NADP^+$ dependent mutant of formate dehydrogenase linked to a NADPH-
711 reductase, in the whole-cell reduction of pentafluoroacetophenone. In their
712 case, however, the activity of the oxidoreductase was almost not affected by the
713 fusion.

714 A different genetic engineering approach was taken by Kim et al. (8)
715 and by Lian and coworkers (13) that constructed pyruvate decarboxylase
716 mutant yeasts strains as starting point to develop high titer producers of 2,3-
717 butanediol. Thus, more than 96.2 g/L of 2,3-butanediol by fed-batch
718 fermentation with glucose (8) and more than 100 g/L of (2*R*,3*R*)-2,3-BD, from
719 glucose and galactose were obtained (13). However, those engineered strains
720 did not produce (2*R*,3*R*)-2,3-pentanediol, (2*R*,3*R*)-2,3-hexanediol nor (3*R*,4*R*)-
721 3,4-hexanediol.

722 We also studied the specificity of Bdh1p towards the two hydroxy
723 groups of (2*R*,3*R*)-2,3-pentanediol and (2*R*,3*R*)-2,3-hexanediol upon oxidation

724 with NAD^+, as well as for the reverse reaction, the reduction of 2,3-
725 pentanedione and 2,3-hexanedione with NADH. The reduction of 2,3-
726 pentanedione after one hour of reaction yielded (3*R*)-hydroxy-2-pentanone as
727 intermediate (Fig. 7A). When the reduction reaction was complete (Fig. 7B), the
728 selectivity was studied in the oxidation direction, yielding (2*R*)-hydroxy-3-
729 pentanone. Furthermore, we prepared the four 2,3-pentanediol stereoisomers
730 by borohydride reduction of 2,3-pentanedione finding that the most abundant
731 species (from their NMR signals) were the enantiomeric pair (2*R*,3*S*)-2,3-
732 pentanediol and (2*S*,3*R*)-2,3-pentanediol (supplemental Figure S1), that when
733 loaded into the chiral column yielded the two more abundant peaks with longer
734 retention times (supplemental Figure S2). To characterize the configurations of
735 these two stereoisomers, we reduced 2,3-pentanedione with Ara1p (the aldo-
736 keto reductase AKR31C) that produced (2*S*)-hydroxy-3-pentanone (our work,
737 reference 33). The reduction of this hydroxyketone with Bdh1p gave a single
738 peak, that given the stereoselectivty of Bdh1p should be (2*S*,3*R*)-2,3-
739 pentanediol, with a retention time of t_R=16.87 minutes (results not shown).
740 Consequently, we could assign the remaining peak at t_R=16.63 minutes to
741 (2*R*,3*S*)-2,3-pentanediol. The identity of the peaks eluting at t_R=14.86 and
742 t_R=15.51 was assigned from the reduction of 2,3-pentanedione with Bdh1p,
743 obtaining only one stereoisomer that corresponds to the one eluting at t_R=15.51
744 minutes (supplemental Figure S3). After our previous discussion (see above),
745 we can safely assume that this stereoisomer should be (2*R*, 3*R*)-2,3-
746 pentanediol and the one eluting at t_R=14.86, should then be (2*S*,3*S*)-2,3-
747 pentanediol. Upon oxidation of the mixture of the four 2,3-pentanediol
748 stereoisomers, it can be observed that the most reactive species were (2*R*,3*R*)-

749 2,3-pentanediol and (2*S*,3*R*)-2,3-pentanediol (supplemental Figure S8) yielding
750 (2*R*)-hydroxy-3-pentanone and (2*S*)-hydroxy-3-pentanone, indicating the
751 preference towards the oxidation of the most internal carbon with *R*
752 configuration.

753 A consistent result with these observations was obtained when
754 studying the oxidation/reduction of (2*R*,3*R*)-2,3-hexanediol/2,3-hexanedione by
755 Bdh1p. The enzyme showed preference for the functional group bound to the
756 most internal carbon, namely C-3, in the oxidation and reduction reactions (Fig.
757 8). Thus, 3-hydroxy-2-hexanone was identified in the reduction direction and 2-
758 hydroxy-3-hexanone in the oxidation direction by its mass spectra. With the
759 characterization of all these intermediates and products, we propose the
760 mechanism shown in Fig. 9, which indicates that the most internal carbon (C-3
761 for 2,3-pentanedione and hexanedione) is the most reactive, since it is the one
762 that predominantly reacts in both directions. Although we did not detect (2*R*)-
763 hydroxy-3-pentanone in the reduction direction of 2,3-pentanedione by Bdh1p
764 (Fig.7A), it would be difficult to discard it completely (Fig. 9 discontinuous line).
765 For the same reason, we draw a discontinuous line in the oxidation of (2*R*,3*R*)-
766 2,3-pentanediol to (3*R*)-hydroxy-2-pentanone, that is much less important than
767 the oxidation of (2*R*,3*R*)-2,3-pentanediol to (2*R*)-hydroxy-3-pentanone
768 (supplemental Figure S8). Since no 3D structure of any (2*R*,3*R*)-2,3-butanediol
769 dehydrogenase has been published yet, it would be speculative to give a
770 structural reason for this preference. A recent article (38) reports the
771 crystallization of the orthologous (2*R*,3*R*)-2,3-butanediol dehydrogenase from
772 *Bacillus coagulans*, therefore we will be able to discuss more deeply the

differential reactivity of both stereogenic centers, once the 3D structure of the enzyme is solved.

Finally, we showed the resolution power of the β-cyclodextrin column that was able to resolve the four hydroxyketones derived from 2,3-pentanedione and the four derived from the 2,3-hexanedione (Fig 10). Although *R*-3-hydroxy-2-pentanone and *R*-2-hydroxy-3-pentanone are not completely resolved with the chiral column under the conditions used, we obtained a better resolution and confirmed their identities by the use of an HP-5MS column (results not shown).

Acknowledgments

The invaluable technical help from Dr. Sílvia Bronsoms from the IBB (Universitat Autònoma de Barcelona) and from Drs. Alba Eustaquio, Maria J. Bergé and Sandra Izquierdo from the Servei d'Anàlisi Química (Universitat Autònoma de Barcelona) are acknowledged. We also thank the "Servei de Ressonància Magnètica Nuclear" (Universitat Autònoma de Barcelona), for allocating instrument time to this project. This work was supported by the grants BIO-2007-64659 from the Ministry of Education and Science (Spain) and (2009 SGR795) from Generalitat de Catalunya (Spain).

References.

1. **Zeng AP, Sabra W.** 2011. Microbial production of diols as platform chemicals: recent progresses.
Curr Opin Biotechnol. **22**:749-57.

797 2. **Ji XJ, Huang H, Ouyang PK.** 2011. Microbial 2,3-butanediol production: a
798 state-of-the-art review.
799 Biotechnol Adv. **29**:351-64.
800 3. **Celińska E, Grajek W.** 2009. Biotechnological production of 2,3-butanediol--
801 current state and prospects.
802 Biotechnol Adv. **27**:715-25.
803 4. **Ma C, Wang A, Qin J, Li L, Ai X, Jiang T, Tang H, Xu P**. 2009. Enhanced
804 2,3-butanediol production by Klebsiella pneumoniae SDM.
805 Appl Microbiol Biotechnol.; **82**: 49-57.
806 5. **Xu Y, Chu H, Gao C, Tao F, Zhou Z, Li K, Li L, Ma C, Xu P.** 2014.
807 Systematic metabolic engineering of Escherichia coli for high-yield production of
808 fuel bio-chemical 2,3-butanediol.
809 Metab Eng..**23**:22-33.
810 6. **Yang T, Rao Z, Zhang X, Xu M, Xu Z, Yang ST**. 2015. Enhanced 2,3-
811 butanediol production from biodiesel-derived glycerol by engineering of cofactor
812 regeneration and manipulating carbon flux in Bacillus amyloliquefaciens.
813 Microb. Cell Fact ; **14**:122.
814 7. **Köpke M, Gerth ML, Maddock DJ, Mueller AP, Liew F, Simpson SD,**
815 **Patrick WM.** 2014. Reconstruction of an acetogenic 2,3-butanediol pathway
816 involving a novel NADPH-dependent primary-secondary alcohol
817 dehydrogenase.
818 Appl Environ Microbiol.; **80**:3394-403.
819 8. **Kim SJ, Seo SO, Jin YS, Seo JH.** 2013. Production of 2,3-butanediol by
820 engineered Saccharomyces cerevisiae.
821 Bioresour Technol. **146**:274-281.

822 9. **Kim SJ, Seo SO, Park YC, Jin YS, Seo JH.** 2014. Production of 2,3-
823 butanediol from xylose by engineered Saccharomyces cerevisiae.
824 J Biotechnol. **192**:376-382.
825 10. **Rong Liu, Hans-Erik Högberg.** 2001. Chemoenzymatic preparation of
826 (2S,3S)- and (2R,3R)-2,3-butanediols and their esters from mixtures of d,l- and
827 meso-diols,
828 Tetrahedron: Asymmetry.**12**: 771-778.
829 11. **Häßler T, Schieder D, Pfaller R, Faulstich M, Sieber V**. 2012. Enhanced
830 fed-batch fermentation of 2,3-butanediol by Paenibacillus polymyxa DSM 365.
831 Bioresour Technol.; **124**:237-44.
832 12. **Yan Y, Lee CC, Liao JC.** 2009. Enantioselective synthesis of pure (R,R)-
833 2,3-butanediol in Escherichia coli with stereospecific secondary alcohol
834 dehydrogenases.
835 Org Biomol Chem. **7**:3914-7.
836 13. **Lian J, Chao R, Zhao H.** 2014. Metabolic engineering of a Saccharomyces
837 cerevisiae strain capable of simultaneously utilizing glucose and galactose to
838 produce enantiopure (2R,3R)-butanediol.
839 Metab Eng. **23**:92-9.
840 14. **Wang Y, Li L, Ma C, Gao C, Tao F, Xu P**. 2013. Engineering of cofactor
841 regeneration enhances (2S,3S)-2,3-butanediol production from diacetyl.
842 Sci Rep.; **3**:2643.
843 15. **Li ZJ, Jian J, Wei XX, Shen XW, Chen GQ**. 2010. Microbial production of
844 meso-2,3-butanediol by metabolically engineered Escherichia coli under low
845 oxygen condition.
846 Appl Microbiol Biotechnol.; **87**:2001-9.

847 16. **Otagiri M, Ui S, Takusagawa Y, Ohtsuki T, Kurisu G, Kusunoki M.** 2010.
848 Structural basis for chiral substrate recognition by two 2,3-butanediol
849 dehydrogenases.
850 FEBS Lett. **584**:219-23.
851 17. **Kaluzna IA, Matsuda T, Sewell AK, Stewart JD.** 2004**.** Systematic
852 investigation of Saccharomyces cerevisiae enzymes catalyzing carbonyl
853 reductions.
854 J Am Chem Soc. **126**:12827-32.
855 18. **Xiao Z, Lv C, Gao C, Qin J, Ma C, Liu Z, Liu P, Li L, Xu P.** 2010. A novel
856 whole-cell biocatalyst with NAD+ regeneration for production of chiral
857 chemicals.
858 PLoS One. **5**: e8860.
859 19. **González, E., M. R. Fernández, C. Larroy, L. Solá, M. A. Pericás, X.**
860 **Parés, and J. A. Biosca.** 2000. Characterization of a (2*R*,3*R*)-2,3-butanediol
861 dehydrogenase as the *Saccharomyces cerevisiae YAL060W* gene product.
862 Disruption and induction of the gene.
863 J. Biol. Chem. **275:**35876-*35885.*
864 20. **González E, Fernández MR, Marco D, Calam E, Sumoy L, Parés X,**
865 **Dequin S, Biosca JA.** 2010. Role of *Saccharomyces cerevisiae*
866 oxidoreductases Bdh1p and Ara1p in the metabolism of acetoin and 2,3-
867 butanediol.
868 Appl Environ Microbiol. **76**:670-9.
869 21. **Storici F, Lewis LK, Resnick MA.** 2001. In vivo site-directed mutagenesis
870 using oligonucleotides.
871 Nat Biotechnol. **19**:773-6.

872 22. **Winston F, Dollard C, Ricupero-Hovasse SL.** 1995. Construction of a set
873 of convenient *Saccharomyces cerevisiae* strains that are isogenic to S288C.
874 Yeast **11**: 53-5.
875 23. **Ito H, Fukuda Y, Murata K, Kimura A.** 1983. Transformation of intact yeast
876 cells treated with alkali cations.
877 J Bacteriol. **153**:163-8.
878 24. **Wach A, Brachat A, Pöhlmann R, Philippsen P.** 1994. New heterologous
879 modules for classical or PCR-based gene disruptions in
880 Saccharomyces cerevisiae.
881 Yeast. **10**:1793-808.
882 25. **Goldstein AL, McCusker JH**. 1999. Three new dominant drug resistance
883 cassettes for gene disruption in *Saccharomyces cerevisiae*.
884 Yeast. **15**:1541-53.
885 26. **Sambrook, J., E.F. Fritsch, and T. Maniatis.** 1989. *Molecular cloning. A*
886 *laboratory manual.* 2nd edn., Cold Spring Harbor Laboratory, Cold Spring Harbor
887 NY.
888 27. **Boeke JD, Trueheart J, Natsoulis G, Fink GR.** 1987. 5-Fluoroorotic acid
889 as a selective agent in yeast molecular genetics.
890 Methods Enzymol.; **154**:164-75.
891 28. **Cordeiro C, Freire AP.** 1995. Digitonin permeabilization of Saccharomyces
892 cerevisiae cells for *in situ* enzyme assay.
893 Anal Biochem. **229**:145-8.
894 29. **Woodyer, R.D., Johannes, T.W. and Zhao, H.** 2006. Regeneration of
895 Cofactors in Enzyme Biocatalysis in “Enzyme Technology” Eds.Pandey, A.,
896 Webb, C., Soccol, C.R. and Laroche C. Springer Science pgs. 83-100

30. **Michnick S., J.L. Roustan, F. Remize, P. Barre, and S. Dequin.** 1997. Modulation of glycerol and ethanol yields during alcoholic fermentation in *Saccharomyces cerevisiae* strains overexpressed or disrupted for *GPD1* encoding glycerol 3-phosphate dehydrogenase. Yeast **13:**783-93.

31. **Enders, D. and Nakai, S.** (1991), Regio-, Diastereo-, and Enantioselective Synthesis of vic-Diols via α-Silyl Ketones According to the SAMP/RAMP Hydrazone Method.
Chem. Ber., **124**: 219–226.

32. **Höckelmann, C. and Jüttner, F.** 2005. Off-flavours in water: hydroxyketones and β-ionone derivatives as new odour compounds of freshwater cyanobacteria.
Flavour Fragr. J. **20**: 387–394.

33. **Calam E, Porté S, Fernández MR, Farrés J, Parés X, Biosca JA.** 2013. Biocatalytic production of alpha-hydroxy ketones and vicinal diols by yeast and human aldo-keto reductases.
Chem Biol Interact. **202**:195-203.

34. **Schröder, F., Fettköther, R., Noldt, U., Dettner, K., König, W.A.and Francke, W.** 1994. Synthesis of (3R)-3-Hydroxy-2-Hexanone, (2R,3R)-2,3-hexanediol and (2S,3R)-2,3-hexanediol, the Male Sex Pheromone of Hylotrupes bajulus and *Pyrrhidium sanguineum* (cerambycidae).
Liebigs Ann. Chem.1211-1218.

35. **Serov AE, Popova AS, Fedorchuk VV, Tishkov VI.** 2002. Engineering of coenzyme specificity of formate dehydrogenase from Saccharomyces cerevisiae.
Biochem J. **367**: 841-7.

922 36. **Schirwitz K, Schmidt A, Lamzin VS.** 2007. High-resolution structures of
923 formate dehydrogenase from Candida boidinii.
924 Protein Sci. **16**:1146-56.
925 37. **Hölsch K, Weuster-Botz D.** 2010. Enantioselective reduction of prochiral
926 ketones by engineered bifunctional fusion proteins.
927 Biotechnol Appl Biochem. **56**:131-40.
928 38. **Miao X, Huang X, Zhang G, Zhao X, Zhu X, Dong H.** 2013**.** Crystallization
929 and preliminary X-ray study of a (2R,3R)-2,3-butanediol dehydrogenase from
930 Bacillus coagulans 2-6.
931 Acta Crystallogr Sect F Struct Biol Cryst Commun. **69**:1140-2.
932
933

934 **Table I. List of oligonucleotide primers used.**

935 The restriction sites and self-complementary regions of the primers FPint-Fw

936 and FPint-Rv are underlined.

Function	Name	Sequence
Cloning *FDH1* and *FDH1-BDH1*-6His in vector pYES2	o-FDH-fw	5' CGC GGA TCC AAT ATG TCG AAG GGA AAG G 3'
Cloning *FDH1* in vector pYES2	o-FDH-rv	5' CCG GAA TTC TTA TTT CTT CTG TCC ATA AGC TCT GG 3'
Construction of the template for FDH1-BDH1-6His	FPint-Rv	5' CAA AGC TCT CAT ACC TTG AAA ATA CAA ATT TTC TTT CTT CTG TCC ATA AGC TCT GG 3'
Construction of the template for FDH1-BDH1-6His	FPint-Fw	5' CAG AAG AAA GAA AAT TTG TAT TTT CAA GGT ATG AGA GCT TTG GCA TAT TTC AAG AAG 3'
Cloning FDH1-BDH1-6His in vector pYES2	bdh1-his	5' GCG GAA TTC TTA ATG ATG ATG ATG ATG ATG CTT CAT TTC ACC GTG ATT GTT AGG 3'
Strain generation WV36-405 *URA3-NAT1::*p_{bdh1}*-bdh1*	Pbdh-ura-fw	5' GAG CAG TCG GAA AGA TCA AGA AAG ACT ACG AGA ATC AAT AAA CGA GGC CAA TAC AAC AGA TCA CGT G 3'
Strain generation WV36-405 *URA3-NAT1::*p_{bdh1}*-bdh1*	Bdh-nat1-rv	5' ATT AGT GAA GTG AAT ATC ACC CTT CTT GAA ATA TGC CAA AGC TCT CAT TCG ACA CTG GAT GGC GGC G 3'
Strain generation WV36-405 P_{GAL1}*-BDH1*	Pbdh-gal-Fw	5'GAG CAG TCG GAA AGA TCA AGA AAG ACT ACG AGA ATC AAT AAA CGA GGC ACG GAT TAG AAG CCG CCG AGC 3'
Strain generation WV36-405 P_{GAL1}*-BDH1*	Bdh-gal-bis-rv	5' ATT AGT GAA GTG AAT ATC ACC CTT CTT GAA ATA TGC CAA AGC TCT CAT TAT CCG GGG TTT TTT CTC CTT GAC G 3'
Verification of the construct P_{GAL1}*-BDH1*	o-gal1-fw	5' CCG ACG GAA GAC TCT CCT CCG 3'
Verification of the construct P_{GAL1}*-BDH1*	o-bdh1-rv	5' GGT CCG CAC AAC TGC TGG CAG C 3'

937

Applied and Environmental Microbiology

938 **Table II.**

939 **Steady-state kinetic constants of yeast Bdh1p towards acetoin and**

940 **several vicinal diketones.**

941

942 Acetoin and diketone reduction activities were measured at 25°C in 33 mM

943 sodium phosphate pH 7.0 with 0.2 mM NADH.

944

945

	k_{cat} (s^{-1})	K_M (mM)	k_{cat}/K_M ($s^{-1} \cdot M^{-1}$)
(*R*/*S*)-acetoin	1,625±83	3±0.6	$5.4x10^5 \pm 1.3x10^5$
diacetyl	1,735±165	60±2	$2.9x10^4 \pm 0.4x10^4$
2,3-pentanedione	826±83	33±7	$2.5x10^4 \pm 0.8x10^4$
2,3-hexanedione	55±8	6±3	$9x10^3 \pm 6x10^3$
3,4-hexanedione	22±1	0.7±0.2	$3x10^4 \pm 1x10^4$

946

947 **FIGURE LEGENDS**

948 **Figure 1. Production of diols by purified Bdh1p.**

949 Gas chromatograms obtained after extraction with chloroform of the products
950 obtained from a reaction mixture containing 50 mM diketone, 1 mM NADH, 100
951 mM sodium formate and 4 U of FDH in 33 mM sodium phosphate, pH 7, after
952 the addition of 200 U of pure Bdh1p, together with 1-hexanol as an internal
953 standard. Total reaction time was 20 h.

954

955 **Figure 2. Stereoisomer purity of the (2*R*,3*R*)-2,3-butanediol obtained with**
956 **pure Bdh1p and diacetyl.**

957 Panels A and B correspond to the enlarged region of 2,3-butanediols
958 stereoisomers, before (panel A) and after (panel B) adding external (2*S*,3*S*)-2,3-
959 butanediol and (*meso*)-2,3-butanediol. (A) Enlarged chromatogram
960 corresponding to a reaction with diacetyl, Bdh1p and an NADH-regenerating
961 system where the concentration of the reaction product (2*R*,3*R*)-2,3-butanediol
962 was 13.7 mM.
963 (B) Enlarged chromatogram containing the reaction mixture from panel A, to
964 which (2*S*,3*S*)-2,3-butanediol and (*meso*)-2,3-butanediol were added as
965 controls. The final concentration of (2*R*,3*R*)-2,3-butanediol was 12.9 mM, while
966 the concentrations of (2*S*,3*S*)-2,3-butanediol and (*meso*)-2,3-butanediol were
967 0.1 mM each.

968

969 **Figure 3. Production of diols by yeast extracts overexpressing Bdh1p and**
970 **Fdh1p.**

Gas chromatograms obtained after extraction with chloroform of the products obtained from a reaction mixture containing 50 mM diketone, 1 mM NADH, 100 mM sodium formate in 33 mM sodium phosphate, pH 7, 20 h after the addition of an extract of yeast strain DP-BDH1 containing 3 U of Fdh and 150 U of Bdh, together with 1-hexanol as an internal standard.

Figure 4. Production of diols by permeabilized yeast cells overexpressing Bdh1p and Fdh1p.

Gas chromatograms obtained after extraction with chloroform of the products obtained from a reaction mixture containing 2% galactose, 50 mM diketone, 5 mM NAD^+, 100 mM sodium formate in 33 mM sodium phosphate, pH 7, after the addition of permeabilized DP-BDH1 yeast cells, together with 1-hexanol as an internal standard. Total reaction time was one hour for diacetyl and 2,3-pentanedione and 20 h for 2,3-hexanedione and 3,4-hexanedione.

Figure 5. Determination of the molecular properties of the fusion protein Fdh1p-Bdh1p$(His)_6$.

(A) Western blot analysis of yeast protein extracts developed with an anti-His antibody, Lane 1, Mr standards; lane 2, 15 µg from strain WV36-405*Δara1 Δ bdh1* [pYES2-*FDH1-BDH1*-6His] extract; lane 3, 17 µg from strain WV36-405*Δara1BDH1* [pYES2-*BDH1*-6His] extract; lane 4, 21 µg from strain WV36-405*Δara1 Δbdh1* [pYES2-*BDH1*-6His] extract. (B), IEF gel (pH 3 to 9) stained with 100 mM (2*R*, 3R)-2,3-butanediol. *Lane 1*, pI standards; *lane 2*, 30 mU of butanediol dehydrogenase activity, from strain WV36-405 *Δara1 Δbdh1* [pYES2-*FDH1-BDH1*-6His] extract; *lane 3*, 7 mU of Bdh from a yeast strain

WV36-405 *Δara1 BDH1* [pYES2-*BDH1*-6His] extract; *lane 4*, 6 mU of Bdh from strain WV36-405 *Δara1 Δbdh1* [pYES2-*BDH1*-6His] extract. (C), size exclusion chromatography of purified Bdh1p(His)$_6$ and fusion protein Fdh1p-Bdh1p(His)$_6$ on a SuperDex 200 prep grade column. *a*, β-amylase (200 kDa); *b*, yeast alcohol dehydrogenase (150 kDa); *c*, bovine serum albumin (66 kDa); *d*, carbonic anhydrase (29 kDa); *e*, cytochrome *c* (12.4 kDa).

Figure 6. Stereoisomeric composition of the products obtained from reaction mixtures containing vicinal diketones and purified fusion protein Fdh1p-Bdh1p(His)$_6$.

Stereoisomer composition of the products obtained with a reaction mixture containing purified fusion protein Fhd1p-Bdh1p(His)$_6$, 37 U of Bdh activity and 0.3 U of Fdh activity, 5 mM NAD^+, 100 mM sodium formate, in 33 mM sodium phosphate buffer at pH 7, together with 50 mM of the compounds diacetyl (A), 2,3-pentanedione (B), 2,3-hexanedione (C) and 3,4-hexanedione (D). Total reaction time was 20 h.

Figure 7. Stereoisomeric composition of the products from the reduction/oxidation of 2,3-pentanedione/(2*R*,3*R*)-2,3-pentanediol with Bdh1p.

(A) Stereoisomer composition of the products obtained in a reaction mixture containing Bdh1p, 50 mM 2,3-pentanedione, 1 mM NADH and an NADH-regenerating system (100 mM sodium formate and 1 U of formate dehydrogenase) in 33 mM sodium phosphate, pH 7, after the addition of 40 U of pure Bdh1p, together with 1-hexanol as an internal standard, with a total

reaction time of 1 h. The inset shows the relative abundances of the ions with an *m/z* of 59 (in black) and of 45 (in red), for the peak eluting at 6.1 min from the chiral column.

(B) Stereoisomer composition of the products obtained in a reaction mixture containing Bdh1p, 50 mM 2,3-pentanedione, the same components of reaction solution as A, after the addition of 40 U of pure Bdh1p, together with 1-hexanol as an internal standard, with a total reaction time of 20 h.

(C) Stereoisomer composition of the products obtained in a reaction mixture containing Bdh1p, (2*R*,3*R*)-2,3-pentanediol, 5 mM NAD^+ and a NAD^+-regenerating system (50 mM α-ketoglutarate, 100 mM ammonium chloride and 6 U of glutamate dehydrogenase) in 33 mM sodium phosphate, pH 7, after the addition of 6 U of Bdh1p, together with 1-hexanol as an internal standard, with a total reaction time of 20 h. The inset shows the relative abundances of the ions with an *m/z* of 59 (in black) and of 45 (in red), for the peak eluting at 7.1 min from the chiral column. The differences in retention times were due to running some samples in different days.

Figure 8. Stereoisomeric composition of the products from the reduction/oxidation of 2,3-hexanedione/(2*R*,3*R*)-2,3-hexanediol with Bdh1p.

(A) Stereoisomer composition of the products obtained in a reaction mixture containing Bdh1p, 2,3-hexanedione 50 mM, 1 mM NADH and an NADH-regenerating system (100 mM sodium formate and 3 U of formate dehydrogenase) in 33 mM sodium phosphate, pH 7, after the addition of 40 U of

Applied and Environmental Microbiology

Bdh1p, together with 1-hexanol as an internal standard, with a total reaction time of 20 h.

(B) Stereoisomer composition of the products obtained in a reaction mixture containing Bdh1p and (2*R*,3*R*)-2,3-hexanediol, 5 mM NAD^+ and a NAD^+-regenerating system (50 mM α-ketoglutarate, 100 mM ammonium chloride and 6 U of glutamate dehydrogenase) in 33 mM sodium phosphate, pH 7, after the addition of 6 U of Bdh1p with 1-hexanol as an internal standard, with a total reaction time of 20 h.

(C) Relative abundances of the ions with an *m/z* of 55 (in black) and of 45 (in red), for the peak eluting at 11 min from the chiral column (panel A).

(D) Relative abundancies of the ions with an *m/z* of 45 (in red) and of 55 (in black), for the peak eluting at 10.7 min from the chiral column (panel B).

Figure 9. Reaction schemes for the oxidation and reduction of (2*R*,3*R*)-2,3-pentanediol and 2,3-pentanedione by Bdh1p.

The scheme accounts for the relative abundances of (*R*)-3-hydroxy-2-pentanone and (*R*)-2-hydroxy-3-pentanone in the reduction of 2,3-pentanedione and in the oxidation of (2*R*,3*R*)-2,3-pentanediol with the C-3 position being the most reactive center in both directions. The discontinuous lines correspond to putative pathways, that although not observed, it would be difficult to rule out completely.

Figure 10. Separation of the four hydroxy-pentanones and four hydroxy-hexanones obtained upon racemization and isomerization of the products

obtained from the oxidations of (2*R*,3*R*)-2,3-pentanediol and (2*R*,3*R*)-2,3-hexanediol by Bdh1p.

(A) 40 mM 2,3-pentanedione and 40 mM 2,3-hexanedione were separately reduced by 6 U of Bdh1p in the presence of 1 mM NADH, 100 mM sodium formate and 4 U of formate dehydrogenase from *Candida boidinii*, in 33 mM sodium phosphate buffer pH 7. After 20 h of reaction, the products were recovered by filtration on an Amicon column and the filtrates (containing the (2*R*,3*R*)-2,3-diols) were subjected to an overnight oxidation by 6 U of Bdh1p in the presence of 5 mM NAD^+, 50 mM α-ketoglutarate, 100 mM ammonium chloride and 6 U of glutamate dehydrogenase. The final reaction products were made 1N in NaOH to induce racemization and isomerization and were loaded (after chloroform extraction) on a β-cyclodextrin gas chromatography column coupled to a mass spectrophotometer.

(B) Relative abundances of the ions with an *m/z* of 59 (in black) and of 45 (in red), for the peaks eluting at 5.67, 5.72, 6.16 and 6.27 min from the chiral column, labeled 1, 2, 3 and 4.

(C) Relative abundances of the ions with an *m/z* of 55 (in blue) and of 45 (in red), for the peaks eluting at 9.03, 9.21, 9.59 and 10.31 min from the chiral column, labeled 5, 6, 7 and 8.

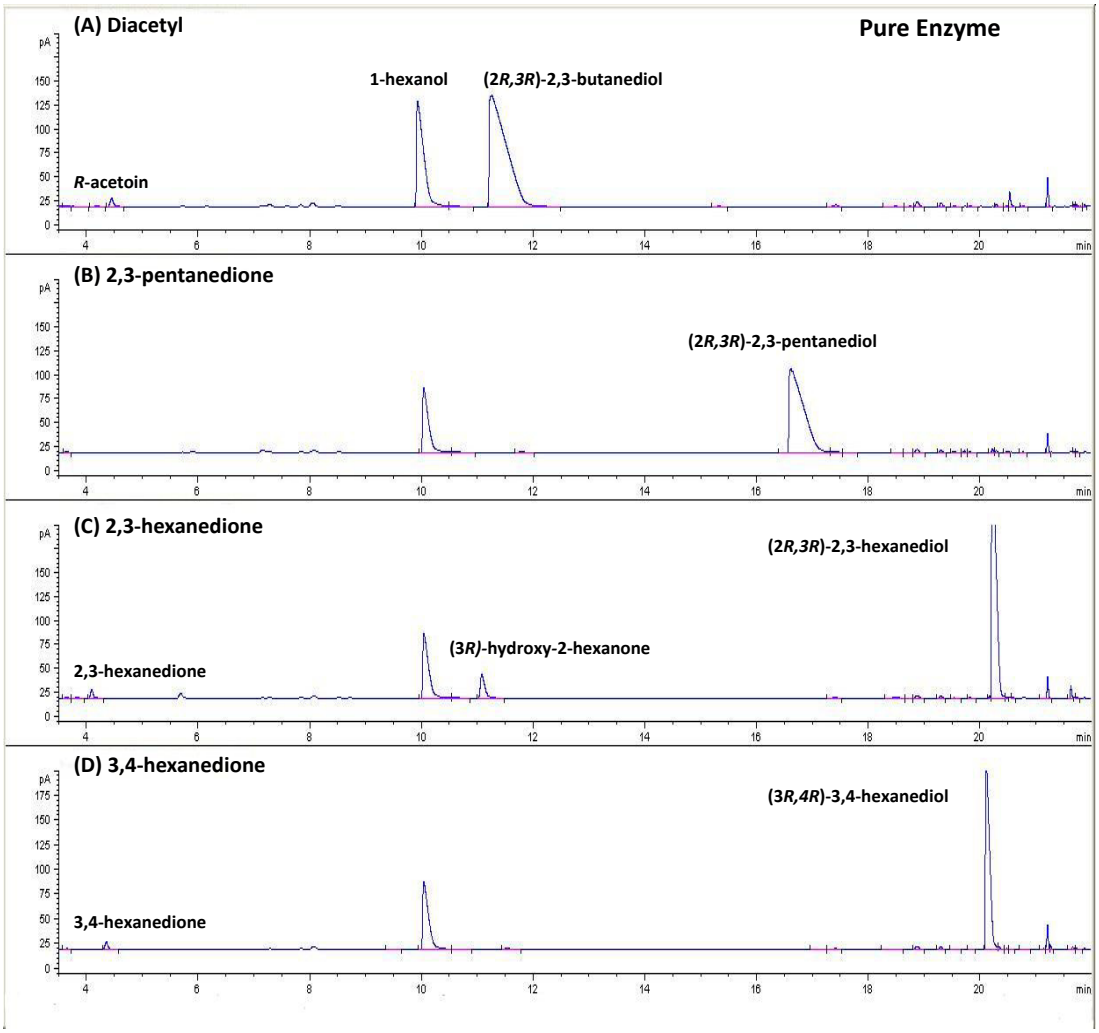

Figure 1

Figure 2

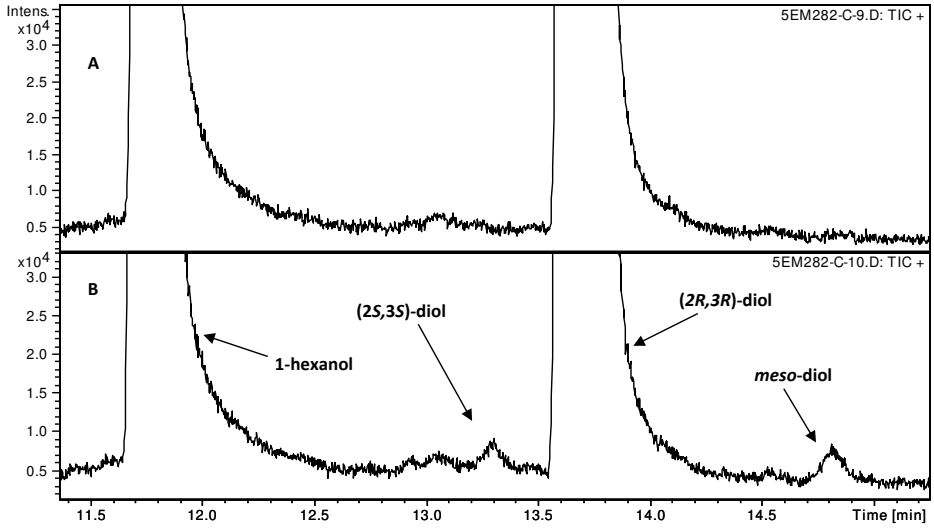

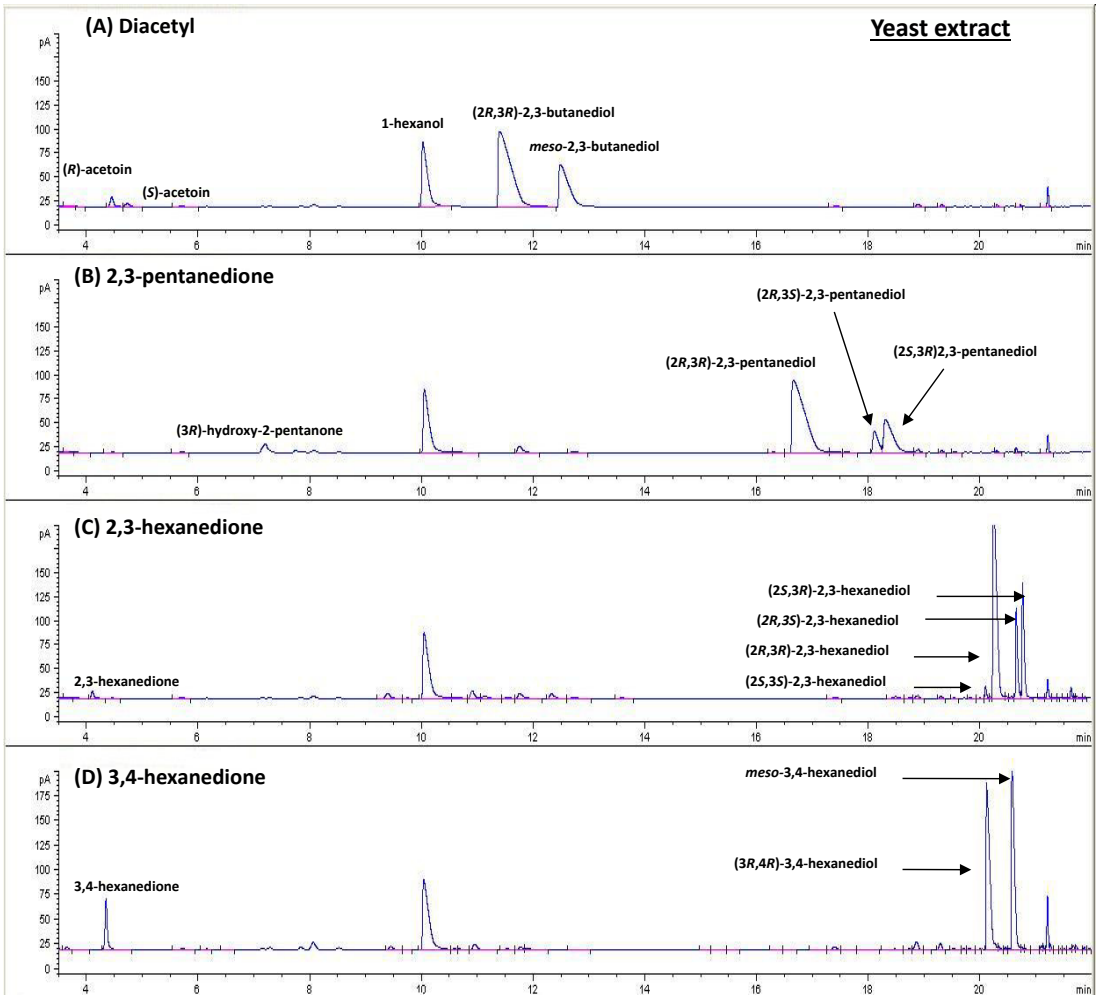

Figure 3

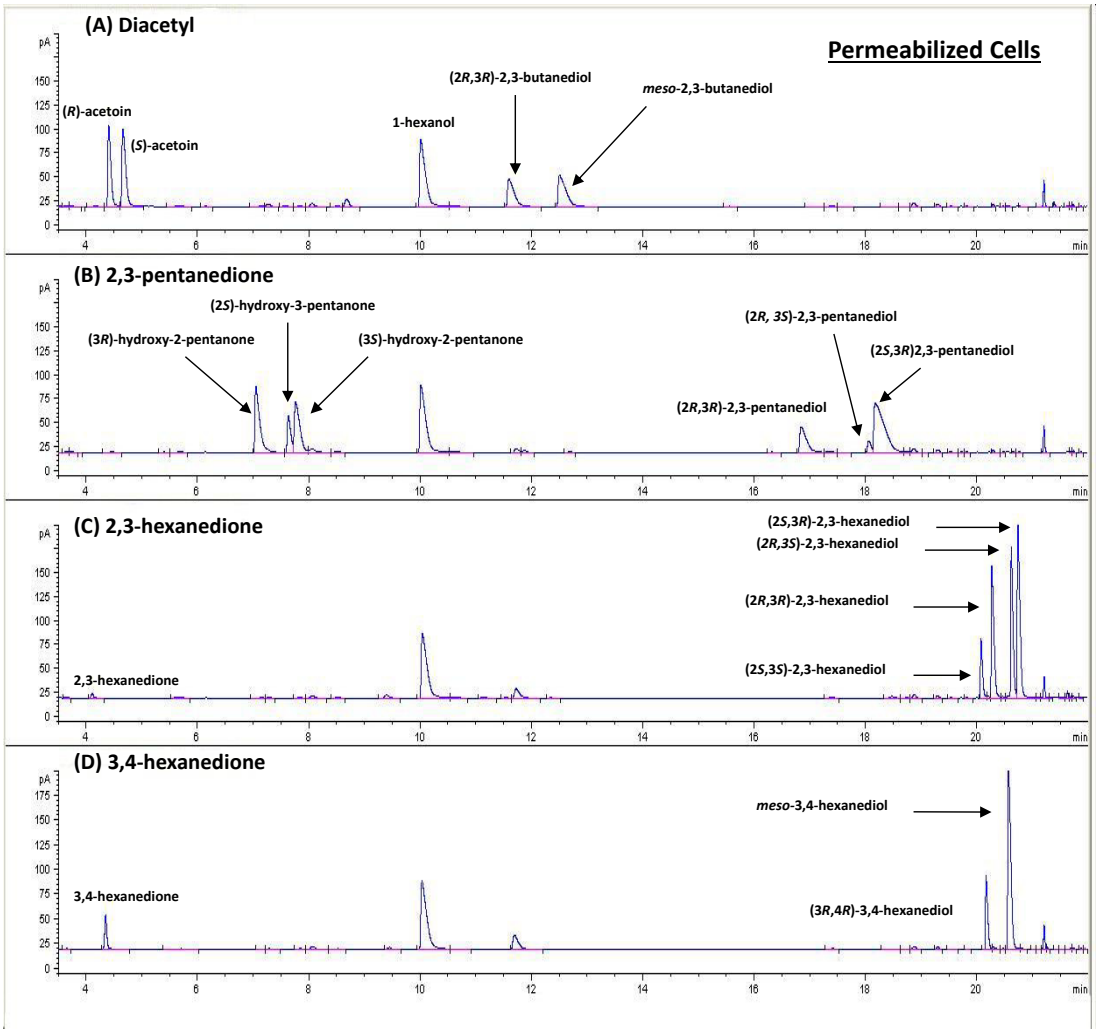

Figure 4

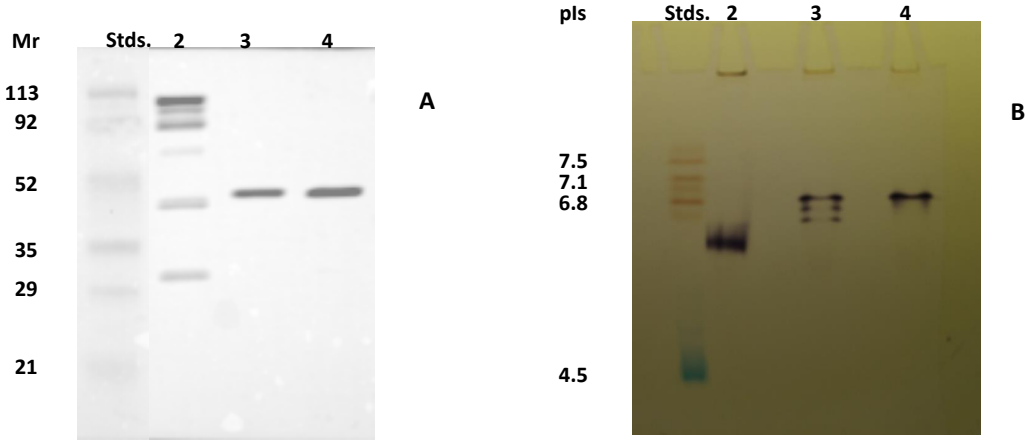

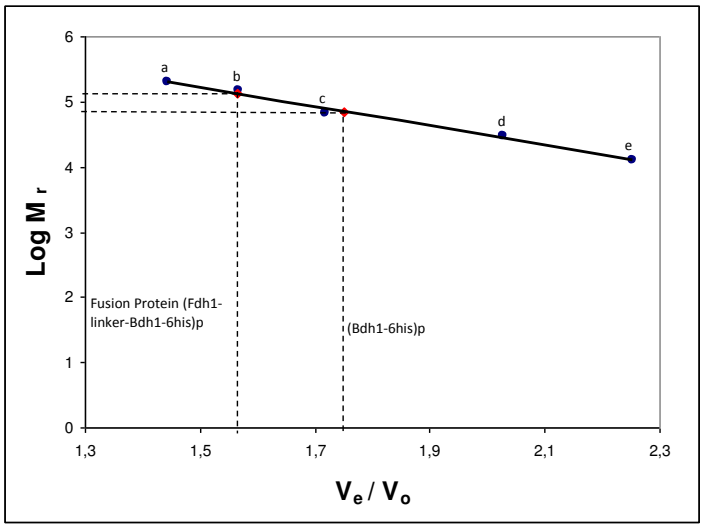

Figure 5

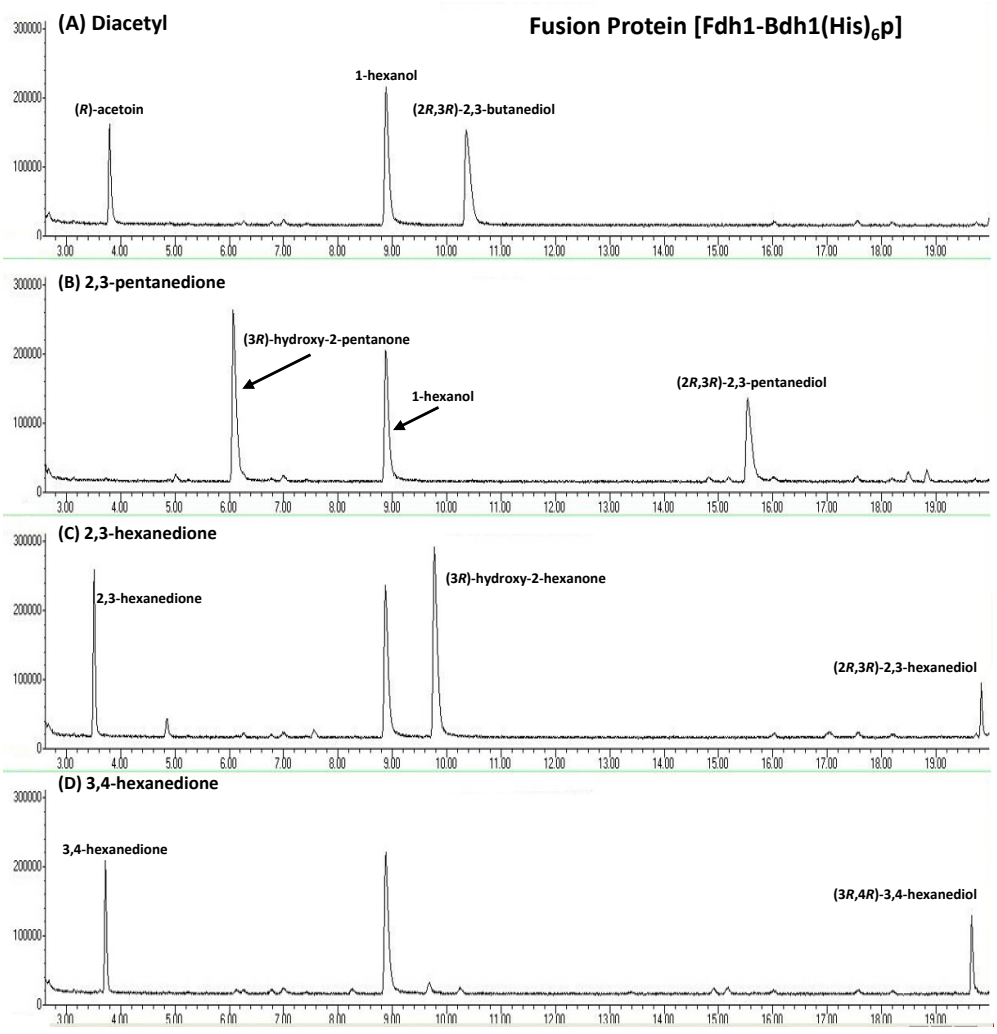

Figure 6

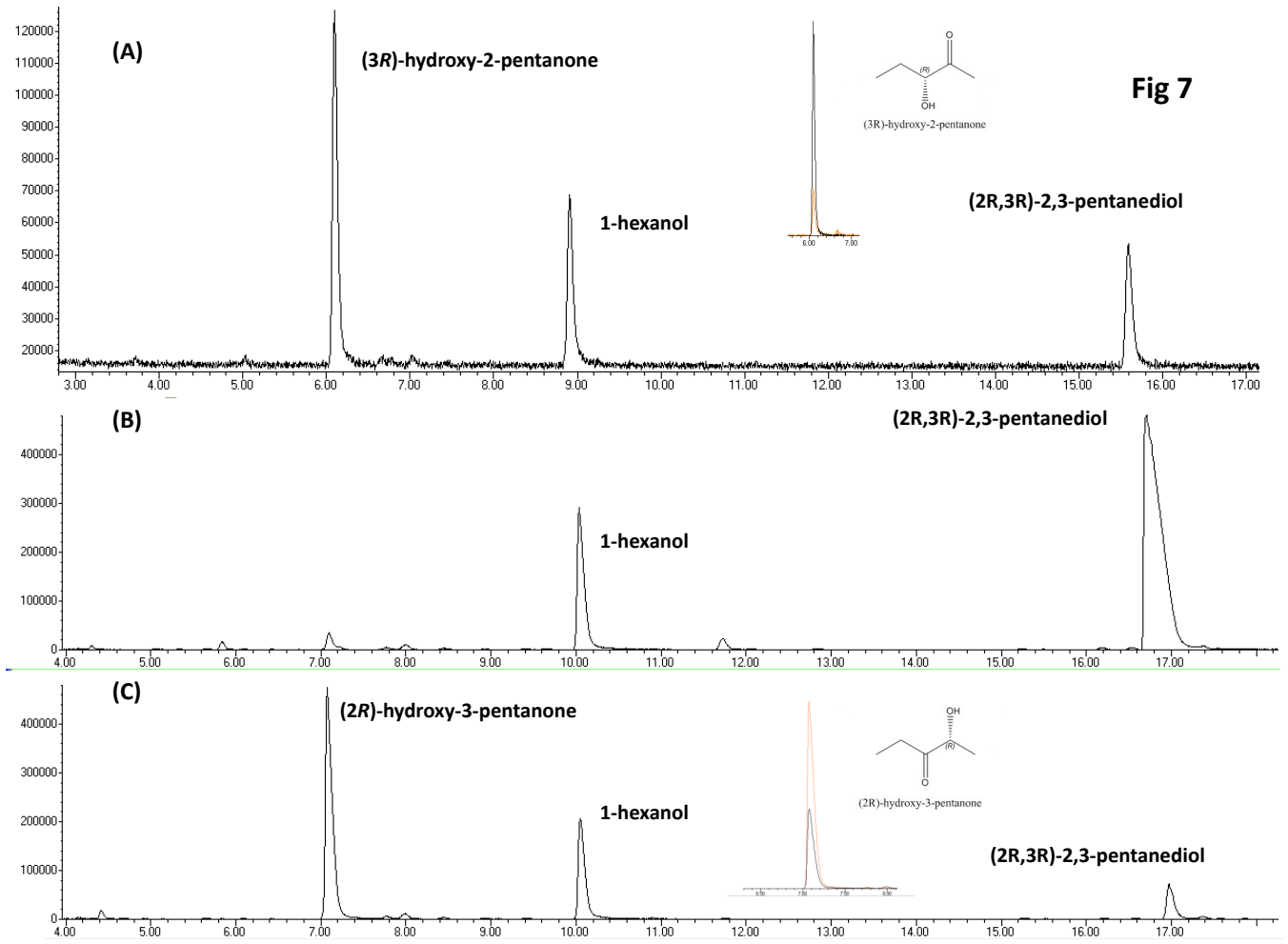

Fig 7

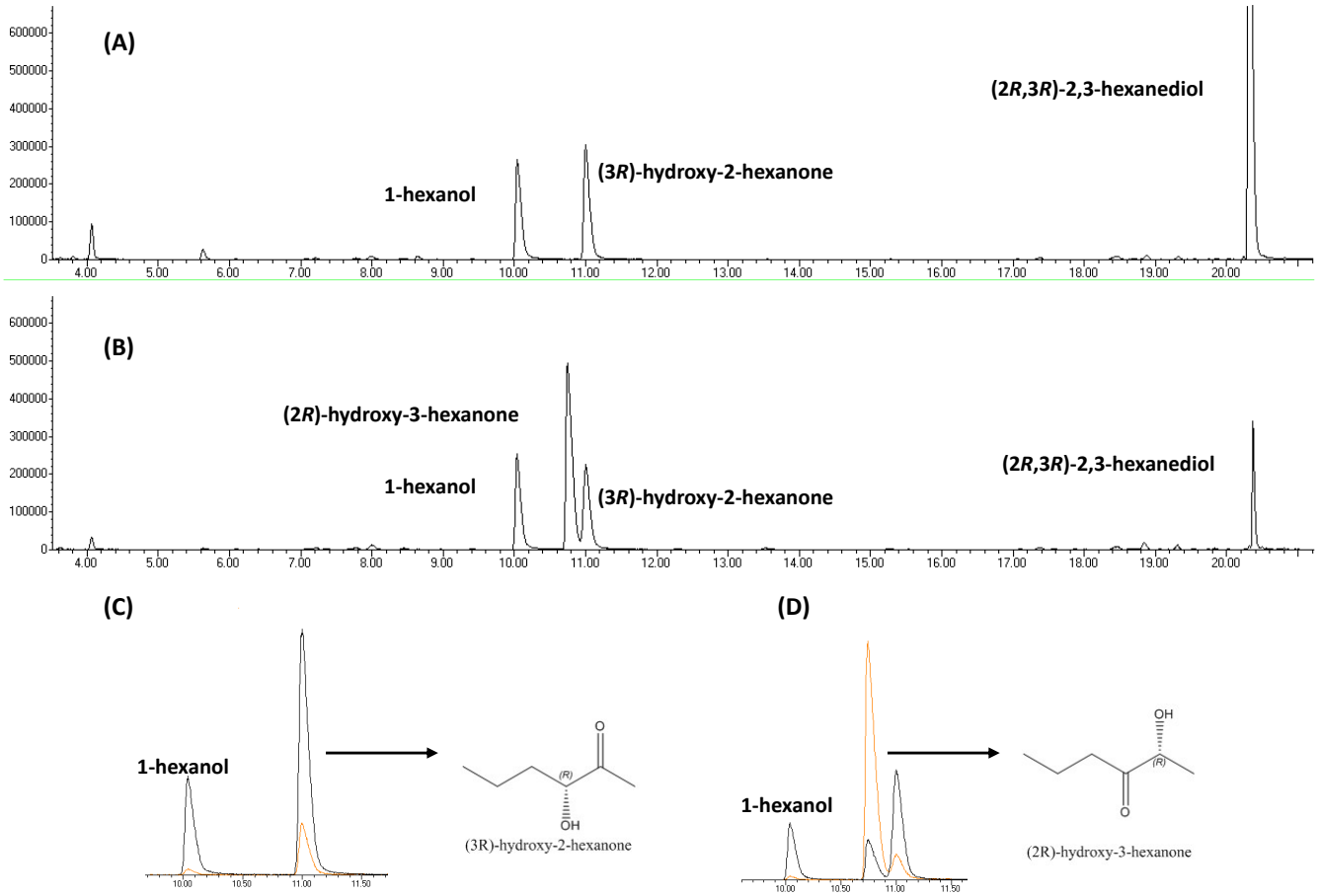

Figure 8

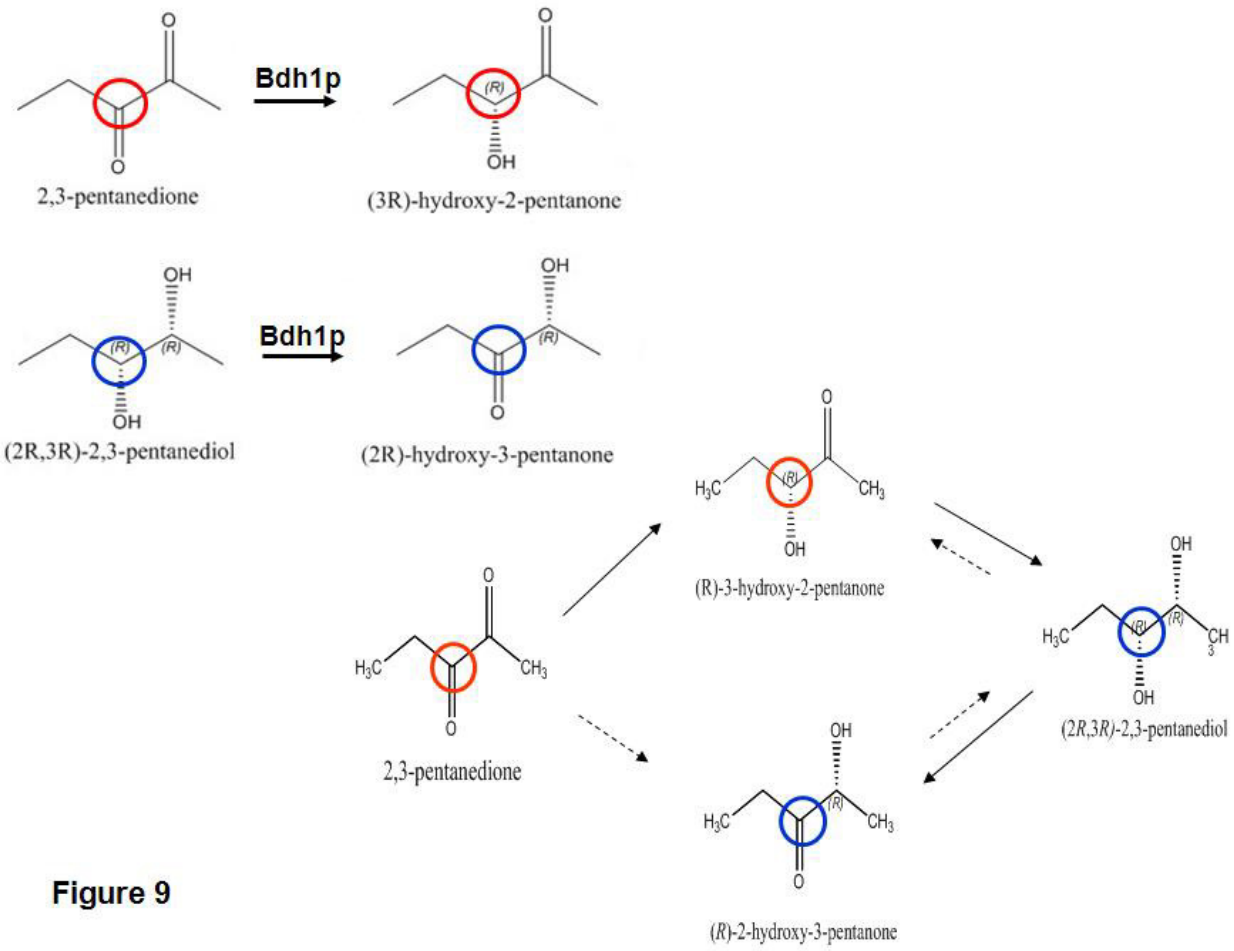

Figure 9

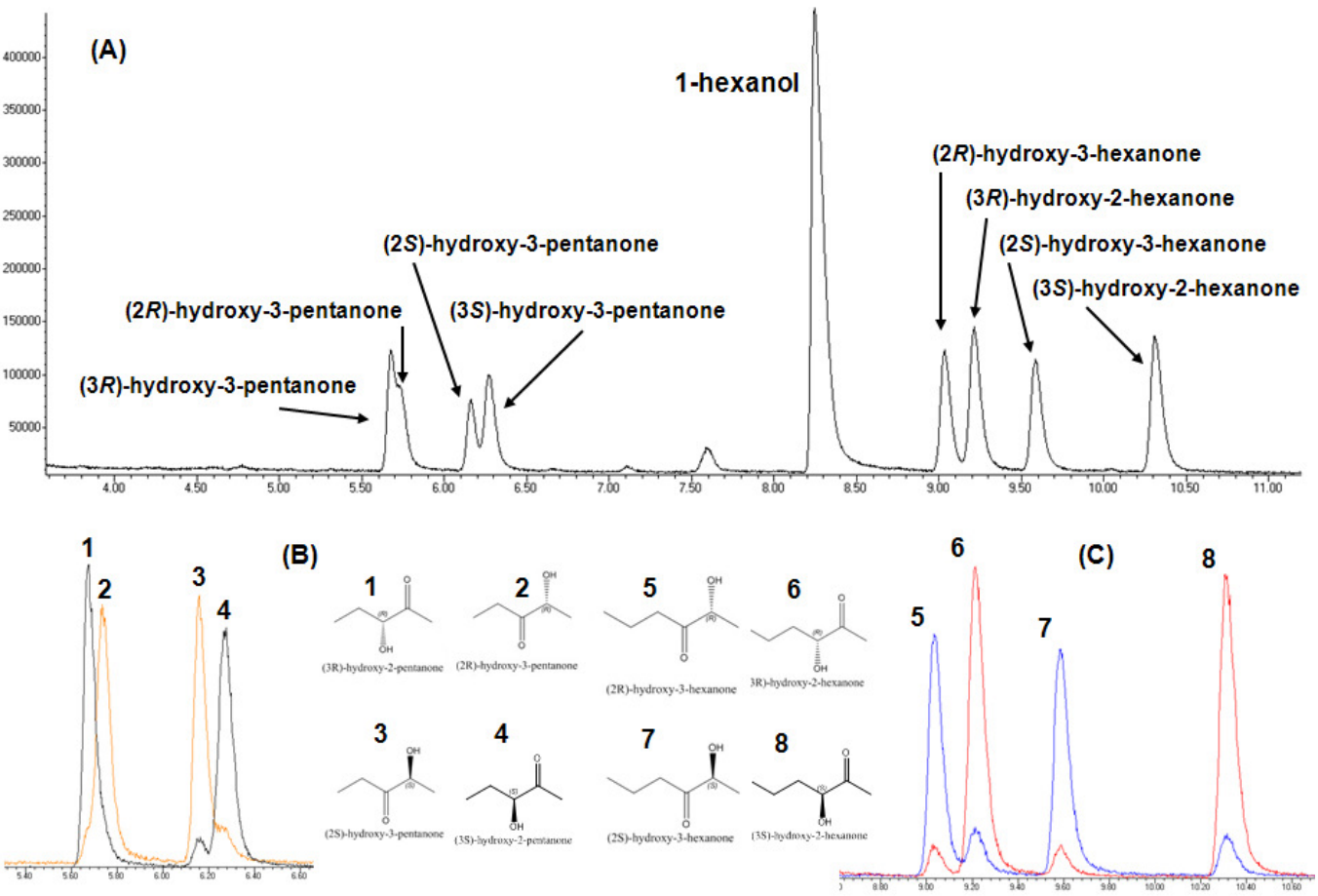

Figure 10